Spring 2023

Speckle Development and Application in UAV-Based Digital Image Correlation for Transportation Infrastructure Monitoring And Assessment

Taylor Wyatt

Speckle Development and Application in UAV-Based Digital Image Correlation for Transportation Infrastructure Monitoring and Assessment

by

Taylor Wyatt

Bachelor of Science in Engineering
University of South Carolina, 2021

Submitted in Partial Fulfillment of the Requirements

For the Degree of Master of Science in

Civil Engineering

College of Engineering and Computing

University of South Carolina

2023

Accepted by:

Dimitris Rizos, Director of Thesis

Nikolaos Vitzilaios, Committee Member

Robert Mullen, Committee Member

Cheryl L. Addy, Interim Vice Provost and Dean of the Graduate School

DEDICATION

This work is dedicated to those in my life who supported me throughout this journey. To my parents and brother who are my biggest cheerleaders. No matter if it was helping me see the big picture, talking me through a stressful moment, or just believing in me when I struggled to. Their unconditional support was invaluable. To my mom for showing me that women can succeed and thrive in STEM. To my roommates and friends who kept me sane and acted as my sounding boards. To my grandparents, aunts, and uncles for their constant support.

ACKNOWLEDGEMENTS

There are several people I would like to thank for their contributions and continued assistance. First and foremost, my advisor Dr. Dimitris Rizos who is the reason for my opportunity and continued dedication to earning my MSc. I could not imagine this process without his steadfast support of me and my work. I would also like to thank my other thesis committee members Dr. Robert Mullen and Dr. Nikolaos Vitzilaios for their invaluable input and critiques. Furthermore, I would like to thank the undergraduate and graduate students who helped me both in the field and the lab. Also, thank you to those at CSX who provided access to their site and monitored our safety on site.

This work has been partially funded by the Federal Railroad Association (FRA) under contract number 693JJ621C000005. The opinions of this work are those solely of the author and are not representative of the those of the FRA.

ABSTRACT

A critical aspect of civil infrastructure is structural health monitoring, of which digital image correlation (DIC) has been proven to be an effective and appropriate method. There is sufficient literature on the use of stationary DIC, but an unexplored aspect is DIC-equipped unmanned aircraft systems. It has been verified in University of South Carolina labs but has not been proved in a field environment. One of the challenges of field implementation is large scale speckle application. This work focusses on identifying and addressing challenges in bringing UAV-DIC technology from the lab to the field. This includes the development of optimized procedures and methodologies for speckle application, specifically on large-scale specimens within civil infrastructure. Various application methods including speckle-by-speckle application, roller with white ink directly onto weathered steel, roller with black ink onto a white background, and printed speckle were tested in terms of feasibility and quality of the pattern. These methods along with the advantages, shortcomings, and potential resolutions are discussed in this work. It was determined that handheld printers used in tandem with guides and painters' tape and different bitmaps on a scrubbed, white painted background were recommended for many applications. Recommendations for future work include investigating the durability of the adherence of the self-adhesive sheets, viability of white ink printed onto the surface, and a speckle pattern printed onto transfer paper.

TABLE OF CONTENTS

LIST OF TABLES

LIST OF FIGURES

LIST OF ABBREVIATIONS

AE ..... Acoustic Emission

AOI ..... Area of Interest

CRP ..... Close-Range Photogrammetry

CWR ..... Continuous Welded Rail

DIC ..... Digital Image Correlation

DOF ..... Depth-of-Field

EKF ..... Extended Kalman Filter

EM ..... Electro-Magnetic

FFT ..... Fast Fourier Transform

FOV ..... Field of View

FRA ..... Federal Railroad Association

GPR ..... Ground Penetrating Radar

GPS ..... Global Positioning System

HRDC ..... High Resolution Digital Cameras

IE ..... Impulse Echo

IMU ..... Inertial Measurement Unit

IoT ..... Internet of Things

IR ..... Impulse Response

LQR ..... Linear Quadratic Regulator

LVDT ..... Linear Variable Differential Transformer

MAV ..... Micro Aerial Vehicle

NCT..... Non-Contacting Technologies

NDT ..... Non-Destructive Technologies

PPE..... Personal Protective Equipment

PWS .....Point-Wise Sensor

QOI ..... Quantities-of-Interest

RNT..... Rail Neutral Temperature

ROI..... Region-of-Interest

SHM..... Structural Health Monitoring

SOD.....Stand-Off Distance

UAS..... Unmanned Aerial System

UPV..... Ultrasonic Pulse Velocity

UsPS..... Ultrasound Proximity Sensors

VSG..... Virtual Strain Gauge

VTOL.....Vertical Take-Off and Landing

WIM..... Wheel Impact Monitors

ZNSSD.....Zero-Mean Normalized Sum of Square Difference

CHAPTER 1
INTRODUCTION

1.1 Problem Statement and Motivation

Transportation networks, such as roadways and railways, are the backbone of society and essential to human health, safety, and economic security and development. Safeguarding the continuous operations of transportation networks enables all other aspects of society to function. Preventing disruption of network operations requires the infrastructure in a state of good repair. Considering that the performance of a structure is its ability to serve the purpose for which it was designed, failure is not necessarily the structural collapse but the inability to function as intended. Performance-based assessment combines vulnerability, risk, and consequence. Therefore, failure to perform leads to a significant impact on the economy, environment, and society due to loss of property and productivity, disruption of service, personal injuries, and even loss of lives. If structural degradation and changes go unnoticed, structures prematurely cease to perform up to standards and are then at risk of catastrophic failure. Detecting structural vulnerabilities is achieved through the implementation of technologies that monitor and assess the condition and performance of the infrastructure and its components, such as bridges, and play a decisive role in intervention through maintenance and repair measures.

Common inspection practices of the transportation infrastructure rely on visual inspections to identify deterioration and damage and assess the current condition. Thus,

they depend heavily on the experience of the inspectors and are highly subjective by nature. More involved practices that focus on monitoring and field-testing activities collect data on the current condition and, for the most part, are dependent on the engineer's judgement, often failing to detect changes in the conditions that can lead to damage. An example of this is the Minnesota I-35W bridge over the Mississippi River collapse in 2007 [1]. Furthermore, they are instrumentation and resource intensive practices which makes it challenging to perform on-demand assessment after extreme events, especially in difficult to reach areas. Capturing early-stage damage or the potential for damage development is one of the great challenges in structural health monitoring and has been the focus of vast research efforts.

Throughout modern history, technological innovations have rapidly progressed from steam- and hydro- powered machines and manufacturing, by incorporating electricity for mass production and assembly lines to computers and automation. Current developments focus on the integration of computers and automation with data and information through artificial intelligence and machine learning, a technological revolution known as Industry 4.0 [2].

Current maintenance strategies are centered around preventative, or condition-based maintenance. As such, the maintenance decision-making protocols are scheduled based on age, usage, and monitoring and inspection data on the current state of the structure. Adopting Industry 4.0 practices in infrastructure monitoring and assessment addresses the challenges in structural health monitoring since it facilitates the development of predictive technologies that will enable performance-based maintenance.

Remote sensing technologies are popular in SHM because it allows for monitoring of structures in difficult to reach locations or positions. It also tends to require fewer work hours and can result in fewer mistakes.

Digital Image Correlation (DIC) is widely recognized as an accurate, non-contacting, and efficient, remote sensing technology, that captures full field shape and surface deformations and has been adopted by several industries. Among the numerous DIC implementations, the technology has proven successful in damage identification, change detection and quality control of railway infrastructure components. Recently, a collaboration between the Advanced Railway Technologies (ART Group) and Unmanned Systems & Robotics Lab (USRL) at the University of South Carolina produced the first implementation of a UAV-based StereoDIC for large structure monitoring [3] [4] [5]. Among the numerous challenges of these developments are: (i) the development of an appropriate speckle pattern for the UAV-based DIC system and (ii) the speckle application method for large-scale structures suitable for UAV-DIC.

1.2 Thesis Objectives

This thesis addresses the challenges regarding the speckle associated with the UAV-based DIC system.

The first objective of the thesis is to understand the operating environment of the UAV-DIC and develop an optimal speckle within the constraints of the data acquisition process and the large scale of the structure. The second objective is to investigate different speckle application techniques considering the field conditions and the relatively large size of the

target area of interest, and identify advantages, shortcomings, and suitability of each technique, in view of speckle application time, durability, and quality.

1.3 Thesis Outline

Chapter 1 – Introduces the importance of structural health monitoring in highway and railway infrastructure, discusses the current and future trends and establishes the motivation, objectives and organization of this thesis.

Chapter 2 – Presents a detailed review and discussion of conventional structural health monitoring methods and the progression into DIC.

Chapter 3 – Explores the fundamentals of DIC including specimen preparation, data acquisition, and data processing.

Chapter 4 – Describes the development and field implementation of the speckle application methods for use by unmanned aerial vehicle (UAV) mounted DIC.

Chapter 5 – Offers a general discussion of the implication, data acquisition, data processing, and quality of work and results. Contains recommendations for future work.

Chapter 6 – Presents the conclusions of the optimal speckle application methods drawn from research.

CHAPTER 2

BRIDGE HEALTH MONITORING AND DIGITAL IMAGE CORRELATION – A LITERATURE REVIEW

The capability to assess the health and behavior of infrastructure, and detect and predict failure, especially in aging structures, is critical to maintain the state of good repair. The focus of condition monitoring is to establish in-service performance of the structure and to detect material degradation, geometry changes, and other deficiencies which can lead to failure. Monitoring also provides valuable information regarding retrofit processes and actions. The family of associated methods and procedures is known as Structural Health Monitoring (SHM). SHM methods for bridge monitoring can be grouped with respect to the location and the level of contact of sensors and data acquisition systems with the monitored structure into three types, i.e., full contact, remote monitoring and non-contacting methods. This chapter presents a discussion of SHM techniques for bridge health monitoring and reviews one class of methods based on optical methods and Digital Image Correlation (DIC) that is the subject of this work.

2.1 Full Contact Methods

Full contact methods require installing the instrumentation and data acquisition systems on the bridge elements and are typically associated with load testing. Full contact methods can be destructive, or non-destructive (NDT) and, in most cases, can be disruptive. Destructive testing involves a temporary service shutdown and at least some maintenance

required afterwards and is typical in testing of bridge components. An example of this is coring for concrete bridges to test for the material's compressive, splitting tensile, and flexural strength [6]. Full contact, non-destructive testing methods include load testing, audio-visual, and stress-wave technologies, and, although temporary service shutdown may be required, do not cause any destruction to the integrity of the structure.

Load testing requires the structure to be loaded under known static or dynamic loads at specific locations without generating a risk of injury or structural damage. The response of the bridge and its components is monitored during testing and deformations are measured by conventional instrumentation attached to the structure. Repeated testing may be conducted for identifying changes in the response over time; while observing signs of damage and/or deterioration [7] [8] [9] [10]. Audio-visual methods are based on manual inspection and are subjective to the individual inspector's interpretation of visual appearance and sound, as seen, for example, in the drag test, and coin tap technique to detect concrete deck delamination or underlying damage in bridge structural elements [6].

Stress-wave methods include acoustic emission (AE), impact echo (IE), sonics, ultrasonic NDT, and impulse response (IR) techniques. The AE technology is often used in the transportation field and is recognized for its ability to identify, locate, and quantify damage [11] [12] [13]. The technique uses transducers attached on the surface of the structure that capture the elastic waves that generate by the rapid energy release when damage initiates and propagates through the structure under observation [6]. AE monitoring is classified as both global (the entire structure) and local (a specific area) monitoring for damage detection [11] [12] [14]. IE testing detects damage and estimates the thickness of a structural member. This is especially useful for crack detection and

measurements. It is based on the same principles as AE with the difference that the waves are generated in the structure through impact loading [6]. The stress pulse waves propagate through the material at a speed determined by the material itself. In the presence of internal defects and external boundaries these waves get reflected and refracted and the propagation path is altered, causing differences in the signals received by the transducers attached to the structure. Processing of the signals in the frequency domain provides the location of the damage or defect within the area. This method is dependent upon the thickness of the structural elements and potential defects may be misinterpreted as element boundaries [6]. Sonic waves techniques are based on similar principles as IE. Ultrasonic pulse velocity (UPV) is an older version of the sonic wave test that identifies the relative condition of concrete by directing an ultrasonic pulse over a known length and recording the time required to reach a transducer [14] [15] [16]. Sonic methods were more common in the past but have lost popularity because they are sensitive to the water content in the structure which affects the wave velocity [6]. Also, they provide relatively low precision measurements compared to the more precise technologies that have been developed that achieve precision in the order of micro-strain. The IR method is also based on the same principles and is often referred to as sonic mobility. In this case, IR methods produce the stress waves using a low-strain impact [6] and determine the mobility and flexibility impulse response spectra of the structure as the ratio of the output to input spectra [17] [18].

2.2 Remote Monitoring

Remote monitoring technologies encompass a broad class of SHM that customarily refers to cases where the structure is monitored in remote locations, often over time, using

different types of wireless sensors attached to the structure. Sensors transmit data to a remote location where data is further processed and evaluated. These methods include wheel impact monitors, electro-magnetic, and close-range-photogrammetry. Wheel impact monitors (WIM) are a remote sensing method of measuring the dynamic forces on railways caused by wheel defects [19]. The WIM includes both strain-based monitors and accelerometer-based monitors. Strain-based WIM measures the strain in the rail web or foot which can in turn be used to determine the load at the rail head. The main benefit of this system is the ability to calibrate the relationship between the applied load and sensor output [19]. This leads to fewer variances and imperfections in the data acquisition. Gauges are often bonded to the web of the rail with the sheer strain determining the applied force [19]. Therefore, despite often being referred to as a non-contacting method, WIM is simply remote rather than fully non-contacting. The gauges still need to be connected to the rail to take measurements and gather data. Accelerometer-based WIM measure the motion over the rail to know the dynamic load that is applied to the rail. A significant advantage of this method is that it can monitor the condition of the entre rail, unlike strain-based which only measures up to 90%. This is because of its ability to measure the impact across the entire length of the rail between two sleepers. This method, like strain-based WIM, is commonly called non-contacting because the data can be viewed remotely but it is not actually non-contacting due to the sensors that must be attached to the structural system. For accelerometer-based, the sensors can be placed on the foot of the rail, under the rail, or below the head and generally at the midpoint between two sleepers [19] [20]. WIM can be used in investigations of train-track-bridge interactions where the system is considered coupled [21].

Electro-magnetic (EM) testing methods are varied but ground penetrating radar (GPR) is the most applicable to this work and can be broken into two categories: remote and non-contacting. Non-contacting GPR will be discussed in a later section. GPR is considered one of the most successful NDT methods used for the inspection of bridge decks and pavements, creating an EM wave reflection survey [6]. Remote GPR is not fully non-contact because it requires ground-coupled antennas that are placed either directly on or very close to the deck surface. Factors that affect the accuracy and effectiveness of GPR are the condition and properties of the asphalt concrete overlay, chloride and moisture content, and level of deterioration. It has been suggested that about 90% of the variation in rebar reflection amplitude is because of fluctuations in concrete cover thickness and the rebar geometrics directly contribute to the other 10%. This means that if the GPR analysis has these discrepancies and causes incorrect predictions and actions, there can be a large, negative cost impact [22].

Close-range photogrammetry (CRP) is another remote testing method that analyzes two-dimensional (2D) information of a reference object to develop the 3D geometry. This lowers the amount of field work required along with the typical completion time [22]. CRP uses a digital camera, topographical equipment, and target points on the bridge to acquire data for a geometric process. The camera must be manually run but can be done from a distance or remotely, but the target points must be on the structure, defining this method as remote. The benefits of CRP are the option for remote viewing, a relatively easy set up process, and lower time and labor requirements than manual inspection [22]. However, this method can be greatly influenced by the environmental conditions at the time of the measurements, such as atmospheric pressure, temperature, and vibrations. Other relevant

determinants are the digital camera matrix resolution, optical system quality, and photogram processing capacity [23]. This photogram processing is the method of using a program to combine individual images.

2.3 Non-Contacting Techniques

Non-contacting testing (NCT) methods include non-contact GPR, terrestrial laser scanner (TLS), infrared thermography (IRT), and radiography. NCT is preferred for sites where it is difficult to attach sensors/monitors and/or access them since the monitoring equipment does not need to be directly connected to the specimen to obtain the necessary data. GPR that is non-contact are air-launched mobile arrays that do not need to be connected to the bridges to gather data. This data is then used to create maps of the bridge decks' corrosion, delamination, and concrete elastic modulus. Unfortunately, the further the sensors are from the ground surface, the poorer the lateral spatial resolution of the GPR data, which, when combined with disparities in data due to material and environmental factors, lowers the beneficial impact of air launched GPR [22]. The accuracy of this form of GPR is between 5 and 15 mm when consistent velocity is assumed but when changes to velocity are considered, the accuracy improves [6].

TLS is a NCT technology that creates "high resolution three-dimension (3D) point clouds of objects within a short duration" [22]. TLS is capable of "3D data collection, topographic surveying, heritage mapping, volume assessment, and as-built surveying of structures" [22]. In studies with the deflection measurements compared to that of linear variable differential transformers (LVDTs), TLS had an error of less than 1.6% and the maximum stress determinations were within 2% of the stress measurements from long gage fiber optic sensors and electric strain gage. Therefore, while TLS needs to be manually run,

it is considered an accurate and preferred method to manual inspection. However, for applications requiring sub-millimeter level accuracy, TLS is not recommended because it had variances of up to 3.4 mm when tested in comparison to traditional geodetic techniques [22]. Also, much like close-range-photogrammetry, this method can be influenced by environmental factors including atmospheric pressure, temperature, and vibrations [23].

IRT is consistent in its accuracy and usability that senses the temperature gradient of concrete-pavement surfaces with exposure to either natural or artificial heat [22]. This is necessary because concrete delamination is known to interfere with heat transfer due to lower thermal conductivity so the area above delamination is generally at a higher temperature than the surrounding concrete. With this method, consideration must be made that shallower defects are more heat heavy at the top compared to deeper defects. Also, readings tend to be clearer and more accurate in higher ambient temperature and humidity [22]. The benefit of IRT is that it can analyze a significant amount of surface area in a relatively short period of time. However, the cost of equipment and the impact of environmental effects such as wind speed and moisture can be prohibitive [6]. Therefore, determinations must be informed of possible outside influences on the readings.

Radiography is a method that uses high energy electromagnetic radiation to find reinforcement location, voids in grout and concrete, “material heterogeneity”, layering and honeycombing. When the radiation goes through the member of interest, it is recorded onto photographic film for the investigators to interpret. However, this method is heavily reliant on personnel with specialized training, making it less accessible [6].

Digital Image Correlation is a non-contacting family of methods for acquiring full field shape and deformation measurements and has been implemented in a variety of applications in science and engineering (e.g. [24]). DIC is the NCT method utilized in the experiments and research described in this work and a detailed introduction is discussed in the next section.

2.4 Digital Image Correlation

2.4.1 Historical Development

Digital image correlation (DIC) is a unique suite of non-contacting vision-based full field measurement methods [25] [26]. The first known DIC work was reported as early as 1961 and was originally considered in the photogrammetry family of methods. However, the most significant developments of the technology started in the early 1980's in the UofSC laboratories and over the past four decades the DIC technology flourished and it became a category of its own and has been adopted by various industries. The timeline of the development of the DIC technology is depicted in Table 2.1.

Generally, Stereo-DIC applications are centered around small areas of structures and were popularized for the ability to obtain high-resolution and high accuracy deformation measurements [4]. 3D-DIC technologies can be used for full-field motion and deformation measurements, which are critical to industries such as aerospace, railway, and structures.

2.4.2 Implementations

DIC can be implemented in 2D, or 3D configurations. 2D-DIC uses a single camera system for the measurements while 3D-DIC uses camera pairs and is often referred to as

Table 2.1 History of DIC

Year	Notes	Related Work
1961	Gilbert Hobrough • First known DIC work • Digitally matched features from two perspectives to extract 3D topography	[27]
1982	Ranson and Peters • Extracting local surface deformations from single camera	[28]
1982-1983	McNeill and Sutton • One of the first experiments using 2D-DIC • Single edge cracked specimen undergoing tensile loading	
1983	Sutton • Implementation algorithms for 2D digital image correlation Peters, Ranson, Sutton, Chu, Anderson • 2D-DIC for optical images of rigid body motion	 [29]
1984	He, Sutton, Ranson, Peters • Application of 2D-DIC for optical images of fluid	[30]
1985	Chu et al • First set of validation experiments	[31]
Mid-1980s	2D-DIC is found to be undesirable for most engineering studies	
1986	Sutton • Increased efficiency of computational process	[32]
1987	McNeill et al • Refined fracture experiments	[33]
1988	Sutton • Estimated crack tip stress intensity factor and measurement	[34], [35]
1988-1989	Paquette, McNeill, Sutton • First preliminary StereoDIC experiments were performed • Reconstructed out-of-plane rotation but identified problems	
1989	Bruck, McNeill, Sutton, Peters • Increased computational efficiency • Developed gradient search algorithms	[36]
1992-1993	Sutton, Newman (NASA) • Crack extension in aging aircraft structures	
1993	Luo, Chao, Sutton, Peters • 3D deformation measurement using computer vision	[37]
1994	Luo, Chao, Sutton • Successful experiments for the redeveloped stereovision system • Related to the 88-89 unpublished work	[38]

Year	Notes	Related Work
Late 1980s	Modified StereoDIC system and calibration	
1995	Full-scale airplane test with NASA Langley	
1996	Helm et al • Publication of modified StereoDIC system and calibration	[39]
1997	McNeill, Helm, Lan, Sutton • Surface deformation of aircraft	[40]
2000	Schreier, Braasch, Sutton • Bias due to interpolation of intensity pattern Lu, Cary • Implemented second order displacement gradient	[41] [42]
2002	Schreier, Sutton • Errors due to undermatched subset shape function	[43]
2009	Wang, Sutton, Schreier • Confirmed bias-induced variability	[44]
2011	Wang, Sutton, Ke, Schreier, Reu • Combined stereovision and image matching error equations Ke, Schreier, Sutton, Wang • Published error assessment	[45] [46]
2013	Sutton • Published computer vision-based, non-contacting deformation measurements	[47]
2015	Sutton, Hild • Published advances and perspectives in DIC Ghorbani, Matta, Sutton • DIC for crack mapping of masonry walls	[48] [49]

Stereo-DIC [24]. Three-dimensional digital image correlation (3D-DIC) measure in-plane and out-of-plane full-field deformations, displacements, and rotations on both flat and curved surfaces with a variable field of view [25], while 2D-DIC is limited to in plane measurements and is quite limited in its implementation. For example, 2D-DIC can provide accurate determination of tensile strains and viscoelastic Poisson's ratio, which is important for the structural response of solid propellants [50]. Three-dimensional digital image correlation (3D-DIC) has been widely used in automotive, aerospace, biological, industrial, civil and government and military industries. It is applicable for large and small structures, fluid measurements, aerodynamic loading on flexible wings, and measuring shape and deformation on cylindrical surfaces and balloon structures in the presence of large deformations and rotations, as well as high temperatures [51].

Examples include the widespread applications for large-scale composite structures in industries like: (i) wind energy industry for the analysis of wind turbine blades to validate the finite element models and capability to withstand extreme loading [52] and (ii) aerospace industry for the modal testing of helicopter rotor blades to identify mode shapes or operational deflection shapes [52]. DIC also enables the study of cracking and fracture in structural elements, with specific studies analyzing stress-strain parameters in reinforced concrete structures [53].

Previous work was performed using 3D-DIC for crack-mapping on masonry walls by researchers at the University of South Carolina. The traditional method is the use of point-wise sensors (PWSs) including crack opening gauges, linear potentiometers, and strain gauges. From this information, crack maps are generally hand drawn for various loading steps [49]. The accuracy of the measurements can be influenced by the quality of

the connections to the surface, especially if cracks are forming near the connections or along the gauge length. Furthermore, this method was a safety concern was susceptible to human error as it depended on the inspectors' experience and skill. This study was to implement 3D-DIC for non-contacting method of measurement of full-field deformation of masonry walls to produce detailed, accurate crack maps. To do this, a speckle was applied with dark spray-paint using a polymer stencil placed on the whitewashed, sanded surface [49].

2.4.3 Speckle for DIC Measurements

A critical element of the DIC technology is the application of a high contrast speckle on the surface of the target area. The images of the speckle are captured during data acquisition and are processed within the DIC framework. Thus, the quality of the speckle affects the accuracy and resolution of the shape and deformation measurements. The properties of speckle are contrast, size, speckle density, and speckle edge sharpness. As DIC technology is developed, speckle application has evolved in terms of impact on the accuracy of measurements, application efficiency, and image quality and has been the focus of many research studies.

The creation and application of speckle patterns varies across different industries. The most common methods to create speckle use calligraphy ink, carbide printer toner, graphite powder, and permanent ink marker, as the tint medium to generate the contrast on the specimen surface. The patterns can either be "constructive" or "destructive", defined by whether the pattern is made by adding or taking material from the subject of interest. The destructive methods are usually for measurements in the range of nanometers to micrometers and include scratching, abrading, chemical etching, and focused ion beam

(FIB) milling. Scratching and abrading removes material usually using silicon carbide paper on the surface of an alloy. FIB milling uses a high ion current beam to etch arbitrary shapes for speckle patterning [54]. Constructive methods within the same measurement scale are spin coating, compressed air, and nano-film remodeling. Spin coating is the spreading of a thin axisymmetric film of Newtonian fluid on a planner substrate. It is typically used to create thin, uniform films of photosensitive organic materials. The compressed air method blasts powder through a filter to produce a pattern while filtering out the larger particles. However, there can be problems with the adherence to the surface. Nano-film remodeling uses vapor to alter deposited metal films for analysis. Constructive methods in the order range of millimeters to meters are generally airbrushing or spraying through a stencil or with a spatter-capable machine [54]. When a speckle pattern is not well-defined, there is a problem with image-blurring which can require Gaussian pre-filtering when processing. Soft edge is often obtained using stencils [55].

Overall, there are a variety of methods to apply and assess speckle patterns for different situations and surfaces.

Speckle quality is integral to the accuracy of measurements, so methods for assessing and quantifying the quality are imperative. The four main parameters defining the quality of the speckle are [54]:

1. High contrast (varying grayscale)
2. Randomness
3. Isotropy (no obvious directionality in the pattern)
4. Stability (deforms with the surface)

Visual inspection of the pattern is often insufficient due to potential variance and the dependence on the inspector's knowledge. Mean intensity gradient (MIG) is an established method for quality assessment for contrast and randomness [56]. Mean subset fluctuation is the process of analyzing the variance of necessary subset size across a speckle pattern [57]. As subset size increases, so does the strain precision but the spatial resolution of the data decreases [58]. The importance of and determination of subset sizing will be discussed in later sections. Another method of assessment is Shannon entropy which is from information theory and analyzes the randomness of the pattern; a larger Shannon entropy means higher quality [59]. The standard deviation of gray intensities (SDGIS) within each speckle is another metric for quality assessment [60]. Another method, multi-factor fusion index (MMFI) is advantageous in ultra-high temperature deformation measurements, especially with laser speckle and other artificial speckle. MMFI considers the inhomogeneity of contrast, mean square deviation of gray, and speckle size standard deviation [61]. Convolution neural networks (CNNs) can assess speckle patterns without any related pre-existing qualitative knowledge. CNNs tend to have a higher correlation coefficient with the target than existing measures including MIG, mean subset fluctuation, Shannon entropy, and SDGIS.

2.5 This Work

DIC has been proven effective in a variety of fields and railway infrastructure needs developments in its maintenance and monitoring methods. This, in addition to the incorporation of unmanned aircraft systems, can provide the solution for the needs of the industry, such as easier access to remote sites for inspection. Optimized speckle application

for efficiency and quality is a significant factor in the quality of results. This work focuses on the development of an optimized implementation methodology for speckle application.

CHAPTER 3

DIGITAL IMAGE CORRELATION FUNDAMENTALS

DIC methods acquire digital images of an object over time and store the images in a digital form. Subsequently, image analysis is performed between any pair of images that identify features in a baseline image and match the features in the other images. Tracking the position change of the features across the digital images enables the extraction of full-field surface displacement and deformation measurements. This chapter discusses first the Digital Image Correlation fundamental principles, and the hardware and software needs. Subsequently, the data acquisition process and the data processing steps are outlined.

3.1 Fundamentals of Image Correlation

3.1.1 Requirements

There are two requirements for accurate measurements from DIC: (i) image-specimen correspondence and (ii) image contrast within the local pattern. Correspondence between the image deformation and specimen deformations is achieved when the pattern is fully attached to the surface of the specimen so that the pattern does not detach or deform independently from the specimen. The second requirement of image contrast within the local pattern such that there is contrast within each small subset to accurately identify the local pattern after deformation [62].

Once these requirements are met, other factors influencing the accuracy of measurements include (i) reflective areas (ii) too-large rotations that causes high compression and blurred features within the pixel array and (iii) too-small speckles that are not able to be accurately identified [62].

3.1.2 Feature Identification and Matching

A feature is a local variation of image intensity which the system tracks across sequences of images to obtain measurements. The first image in the process is the reference image. It is an image taken before any deformation or displacement and contains a "set of interrogation points" for the DIC to track. The three methods of selecting a reference image are [24] [62] seen in Table 3.1.

Table 3.1 Reference Image Selection Methods

Method	**Notes**
Single reference image	• Simplest • Typically preferred • Uses reference image of undeformed test piece from beginning of image series • Displacement or motion is tracked by correlating subsequent images to the reference image
Incremental correlation	• Used when DIC pattern experiences significant change to the point that it cannot be correlated to the original reference image • Images are correlated to the one immediately prior rather than the original • Shortcoming: as the amount of images increases, potential error does as well due to total deformation being summed rather than measured
Partitioned correlation	• Compromise between single reference image and incremental correlation • Total image set may be divided into subseries • Each subseries has its own reference image to correlate back to • The deformation of each subseries is summed • Reduces accumulated errors

3.1.3 Speckle Requirements

When using VIC 3D software for image processing for DIC, there are factors that impact the ability to accurately extract displacement and strain data. These factors include [62]:

- At least 40 gray levels within the pattern, constituting high contrast within the images.
- Minimum 3x3 pixel array per feature and enough sampling for accurate reconstruction used in pattern matching.
- Large enough sub-region to have multiple features for optimal pattern matching. The subset generally includes a minimum of three dark and three light features in each direction.

Just as the surface and background need to be relatively smooth, the speckle cannot have a significant texture either as it interferes with the DIC processing. Before applying any speckle, the size must be determined. The physical pixel size of the sensor can be used to determine a rough estimate through experience with what is sufficient. However, the exact size is determined using the lens' properties and distance from the surface. This is done by converting the field of view to pixels and determining the size of a three-by-three set of pixels that a single speckle should cover. This idea is shown in Figure 3.1. The sensors typically measure at 3.5 μm per pixel so the three-by-three set is 10.5 μm by 10.5 μm. This is compared to the physical size determined by the field of view, which is determined by the distance from the surface.

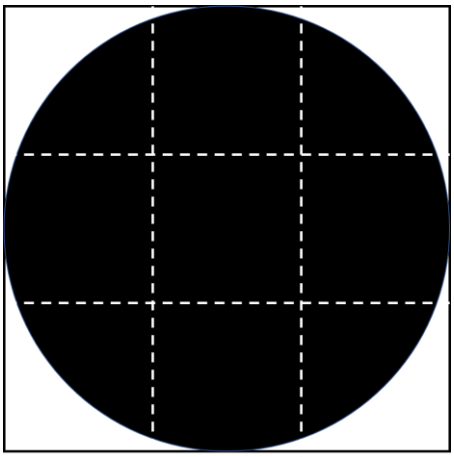

(a)

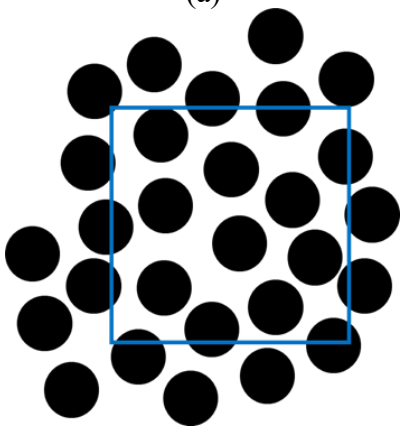

(b)

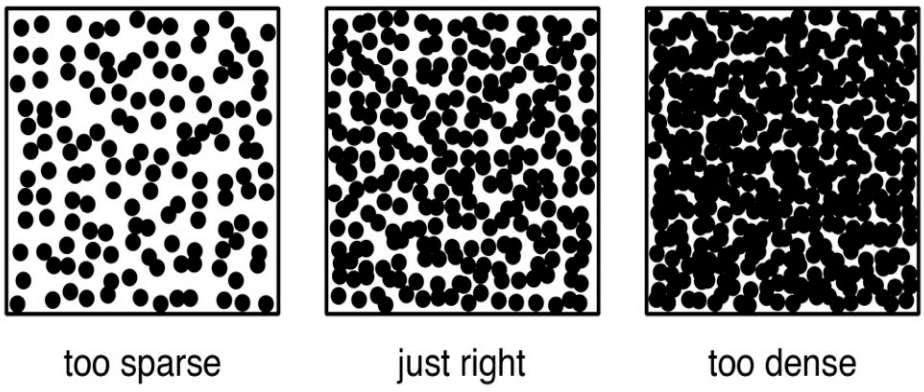

(c)

Figure 3.1 Speckle Development (a) Sample Speckle over 3x3 Pixel Set (b) Sample Subset (c) Varying Speckle Pattern Densities

The mathematical representation of the relationship between camera resolution and specimen field of view in finding the pixel size is seen below [24].

$$resolution = a \times b$$

$$field\ of\ view = c \times d\ (ft)$$

$$per\ pixel = \frac{c}{a} \times \frac{d}{b}$$

The smallest of these two ratios (c/a vs d/b) is then multiplied by three to know the physical size of the pixel set. The diameter of the speckle is then the smallest between the sensor size and the physical size.

A sufficient speckle pattern is imperative when working with DIC for SHM because the quality of the speckle directly impacts the quality of the results. For example, if the pattern varies too much, there can be inconsistencies in the surface measurements and if the speckle density is improper, the subset size will need to be relatively large. This means that there will be fewer data points. If the speckle pattern does not go onto the surface well, the deformation measurements could be incorrect because DIC uses the distinction between the background color (white) and speckle color (black), so, if the speckles are patchy and/or smeared, the program may misread the pattern and either miss deformations or measure deformations that did not happen.

3.2 Typical Stationary System

Traditionally, a stationary system consists of the specimen, speckle pattern, camera(s), camera mounting system, lighting, and a computer for running the relevant software.

3.3 Best Practices

There are six main components of established best practices for DIC measurements [62]:

1. The subset size should contain a minimum of three white and three black features in each direction
2. Subsets should be separated by about 1/3 of the subset size center to center.
3. High contrast is needed to achieve high accuracy, but the pixels should not be saturated.
4. Vibration isolation tables are not necessary, but the specimen-camera system should be stable.
5. In-plane rigid body movement does not cause problems with measurements as long as the specimen remains within the FOV.
6. Laboratory experiments have achieved accuracy up to +/- 0.01 pixels for displacement and +/- 100 με for in-plane strain.

3.4 System Configuration and Pre-Testing Procedures

Once the test expectations and objectives are established and the requirements of the tests and the Quantities of Interest (QOI) to be measured are defined, the decision on the use of a 2D-DIC or 3D-DIC system is made. Typically, a 3D-DIC system is preferable even if 2D-DIC is sufficient for the intended tests unless the test is not able to physically accommodate the multi-camera set up. 2D-DIC tests are assumed to be nominally planar with constant stand-off distance (SOD). Before any data acquisition takes place, several tasks need to be performed. These tasks pertain to system configuration based on testing

needs, specimen preparation, speckle application and system calibration and are discussed below for a 3D-DIC system [24].

3.4.1 Area of Interest (AOI) and Field of View (FOV)

The area of interest (AOI) on the specimen is the area on the surface of the specimen where the full field of deformations is to be measured. The field of view (FOV) of the cameras is determined from the AOI and the expected movements and deformations. The FOV needs to be large enough to cover the extended AOI that includes the region where the AOI may shift to. In a 3D-DIC each camera likely has a separate FOV. The "effective" FOV is defined as the overlap between the FOV of each camera. The effective FOV needs to cover the extended AOI [24].

3.4.2 System Configuration Parameters

Dependent on the geometry of the setup and the highest priority QOI the angle between the lines of sight of the cameras is selected typically between 15° and 35°. Smaller angles yield higher accuracy of the in-plane measurements, but the out-of-plane uncertainty increases. Larger angles allow for higher out-of-plane accuracy of measurements but decreased in-plane accuracy. Once the angle is set the depth-of-field is determined as the distance of the cameras to the specimen that keeps the effective FOV in focus [24].

The expected spatial gradients in the QOI will determine the required spatial resolution of the measurements of the QOI. The measurement resolution and the effective FOV will indicate the minimum required camera resolution and will define the DIC processing parameters such as subset and step size [24].

Acquisition frame rate and exposure time are two parameters that affect the quality of the measurements and need to be estimated before any testing takes place. To this end, the justifiable amount of noise for each QOI intended measurement is specified and is known as the noise-floor. Subsequently, the preferred frame rate for optimal measurement rate and displacement between frames is determined. The maximum allowable exposure rate is defined to limit motion blur. The threshold value of specimen motion between two frames that causes motion blur is usually around 0.01 pixels for typical DIC systems, 0.1-0.3 pixels for machine vision systems, and up to 3 pixels for dynamic modal tests. The exposure time and frame rate are decided independently but the exposure time cannot be greater than the inverse of the frame rate. A typical, conservative calculation is [24] [62]:

$$\frac{\text{allowable specimen motion}}{\text{exposure time}} = \text{noise floor of displacement QOI measurement}$$

Or, alternatively

$$\text{Displacement per exposure [px]} = (\text{Velocity } \left[\frac{\text{mm}}{\text{s}}\right]) \times (\text{Image Scale } \left[\frac{\text{px}}{\text{mm}}\right]) \times (\text{Exposure Time [s]})$$

3.4.4 Camera, Lens, and Lighting Setup

Cameras and lenses are mounted in a way that the desired DOF, effective FOV, and stereo-angle are achieved. Also, both cameras must be mounted together rigidly to avoid relative camera motion. In setting up the cameras and lenses, the following parameters are considered:

- Provide enough degrees of freedom for operators to precisely adjust the location and orientation of the cameras and lenses.

- Have the necessary range of motion and mechanisms to allow for any necessary adjustments for calibration.
- Enable the system to lock once in the final, desired position.
- Mount the system near the center of mass to “minimize the lever-arm effect”.
- Organize cables to keep them from pulling on the cameras are transmitting ambient vibrations to the system.
- Make sure the support structure is stable with any weights needs to prevent motion.
- Make any necessary (and reasonable) efforts to minimize the vibrations transferred to the camera systems.

Once the cameras are mounted the aperture on the lens is set that allows for the desired DOF. The aperture controls how much light is allowed in the system. For stereo-DIC systems, the aperture should be the same, or as close as possible, in each camera. It is noted that:

- As the target DOF increases, the aperture decreases.
- At small apertures, there can be problems with diffraction.
- At large apertures, “optical aberrations are accentuated”.
- “Moderate lens apertures are recommended, to avoid accentuated lens distortions or diffraction limits at extreme apertures.”

Subsequently, aperture is set, and the lighting and exposure time is adjusted to optimize the contrast between the lightest and darkest regions of the pattern. The lighting must be constant and uniform throughout the FOV and time of the test. The following guidelines facilitate the proper setup [24] [62].

- Exposure time must be less than or equal to the maximum exposure time calculated in section 3.4.2
- In some cases, room lighting is sufficient but most of the time, additional lighting is needed to provide quality contrast.
- Cross-polarized or diffuse light rather than focused or spotlight are preferred as they help reduce glare from specular reflections.
- "If the mean contrast in the image changes over time during the test, the zero-mean normalized sum of square difference (ZNSSD) matching criterion is recommended to compensate for contrast changes."
- It is acceptable to adjust lighting between calibration and testing as long as the camera system remains stable.

3.4.3 Camera and Lens Selection

DIC technology uses machine-vision monochromatic cameras with nearly 1:1 pixel aspect ratio. Due to the effect of camera sensor size and lens effect on image scale, the camera and lens cannot be chosen independently. Cameras and lenses are selected based on the DOF, FOV, SOD, noise-floor, spatial resolution, and temporal resolution. Cameras and lenses with automatic adjustments such as of focus or opening/closing apertures with each acquisition are not appropriate and should be avoided in DIC systems [24] [62].

3.4.5 Surface Preparations and Speckle Application

When applying speckle, success is dependent upon the condition of the surface including the texture, cleanliness, and material. All surface types should be as level as possible in terms of unexpected, dramatic dips or bumps. For wooden surfaces, this can make it difficult to apply the methodologies discussed in this paper. Regarding metal

surfaces such as weathered steel, they need to be scrubbed with a wire brush, handheld or mechanical, to remove debris such as dirt or rust which can interfere with the application of paint and/or ink. After the surface debris is scrubbed away, there is generally some loosened debris that remained, so a rag (preferably terry cloth or microfiber) is taken to the surface to wipe away the excess, partially removed debris left by the brush.

The methodology of applying the speckle pattern itself for DIC purposes began with researchers placing each individual mark upon the prepared surface. However, this method is extremely time intensive and can have dramatic variations in sizing and density. A roller or stamp is still a relatively low-cost method and is currently being used for various DIC projects and has been working well. It involves a rubber-like, pre-patterned, stamp on either a slightly curved surface or on a concentric roller depending on the intended uses. Printed self-adhesive sheets are an alternative to the standard methods that require the total pattern to be applied manually. They are sheets that are typically a speckle pattern printed onto matte adhesive paper using run and smear-resistant ink. The use of such sheets is a newly implemented method that was first introduced by researchers at the University of South Carolina.

3.4.6 System Calibration

Once the system is set, pre-calibration is performed. This includes a general equipment cleanliness check, camera warm-up, and synchronization. The camera systems must be turned on to allow sufficient time to reach thermal equilibrium before measurements are taken. As cameras and lights heat with use, they can cause heat waves between the specimen and imaging system, causing errors in the measurements. Synchronization is to ensure the camera systems in stereo-DIC are in synch to avoid delays

between the cameras. Synchronization is most often checked through the epipolar, or projection, error of test images. Pre-calibration also includes checking for glare on the ROI, sub-par pattern, poor contrast, non-uniform lighting, and more. If there are any problems identified during the pre-calibration process, they must be rectified to the best of the researcher's ability.

A calibration target is selected according to the system and test. The calibration target should, preferably, fill the effective FOV but can be as small as about half of the FOV. It is noted that accurate and precise measurements of the feature spacing on the calibration target directly affects the determination of the scaling factors of shape and displacements from the pixel space to physical units. Adjusting lighting may be necessary for calibration, but special attention needs to be paid so as to not jostle the camera system. Acquire a series of images of the calibration target that is rotated about multiple axes and translated horizontally and vertically if the target is smaller than the FOV. The number of calibration images needed is dependent on the software. It is good practice to review the calibration results to try to ensure the quality of future measurements. This includes a review of the parameters such as image center, focal length, and stereo-angles [24].

3.5 Testing Procedures and Data Processing

Researchers at the University of South Carolina have implemented DIC in multiple ways for the monitoring of rail infrastructure within a laboratory environment.

The surface must be properly prepared to ensure sufficient adhesion and texture of speckle. Typically, this is done using a wire brush, handheld or drill-mounted, on a metal surface. There are some situations where a solid-colored background beyond the original surface is necessary. Sometimes the surface must be painted a single, solid color before the

speckle is applied, usually when a light background is wanted to maximize contrast. If such a background is necessary, there are factors that must be considered when choosing and implementing techniques. Some of the following discussion assumes that the desired background is white for the application of a dark (typically black) speckle pattern to maximize contrast. In such cases, the paint used must be flat white to minimize glare and reflection during DIC analysis. While matter white appears nearly indistinguishable to human eyes, it is insufficient when implemented as it results in higher reflection and noise within the data than flat white. The conventional method of applying the background has typically been weather and rust resistant spray paint. Given that the researcher is spraying evenly and at an appropriate distance, a thin but opaque layer with little additional texture can be obtained. Generally, this paint dries relatively quickly but sometimes requires the assistance of a fan to expedite the process, especially if a thicker layer was applied. There are potential problems with opacity and thickness variation as the area of interest and/or environmental wind increased. However, this method is a viable choice for background application if certain requirements are met.

The methodology of applying the speckle pattern itself for DIC purposes began with researchers placing each individual mark upon the prepared surface. This was most commonly done using a sharpie to create precise circles on a white background. Unfortunately, this method is extremely time intensive and can have dramatic variations in sizing and density. So, while the monetary cost of this method is low, the drawbacks make it a much less preferrable option in the field.

3.5.1 Stationary System

During the tests involving a standard stationary system, it was realized that shadows cast from either artificial or natural light sources interfere with the accuracy of the measurements. Thus, the lighting must be consistently monitored and maintained at a consistent level throughout tests to account for any changes. For satisfactory calibration, it is imperative that the target grid is rotated at least as much as the specimen will.

3.5.2 UAS-based DIC System Implementation in Lab

Unmanned Aerial Systems (UASs) have been growing in popularity and applications for structural health monitoring for the accessibility of sites and capability of remote inspections. This is especially true for Vertical Take-Off and Landing (VTOL) Micro Aerial Vehicles (MAV) because of how small they are and the ability to hover in place. This is ideal for remote inspection where minimizing the impact on the structure's and environment is desired. To maximize efficiency and applicability, the drones must be equipped with sufficient imaging capability and the ability to be remotely operated [4].

A paper published in 2021 details research performed at the University of South Carolina where a drone-based Stereo-DIC system was deployed and used in a laboratory environment to judge the validity of application results. The work of Vitzilaios et al. details an Unmanned Aircraft System (UAS) that was equipped with a Stereo-DIC system to collect DIC data of a prestressed railroad tie under loading. UAS are commonly referred to as drones, and in the case of this work, Stereo-DIC-equipped UAS is shortened to DroneDIC. To verify the results, a stationary DIC system was used in tandem with the DroneDIC system to collect comparable data [4].

DroneDIC is a beneficial system because it can combine the accuracy of DIC with the accessibility and maneuverability of drone systems. One of the first implementations of DIC equipped drones was used in 2017 by Reagan et al. but there were considerable challenges with flight instability [4].

To validate the measurements taken with the DroneDIC system, the researchers added LVDT and stationary Stereo-DIC systems much like the early iterations of Chao's work (previously discussed). The LVDT was used to capture deflections at the midspan of the tie [4]. Calibration was performed for both the stationary and UAS-based systems using calibration target images with known scale factors. In the case of DroneDIC, it was calibrated before being airborne, like in the case of the work described in this thesis [4]. Through this work, it was realized that images taken from an UAS cannot be averaged while processing the data in an effort to reduce noise.

CHAPTER 4

DEVELOPMENTS AND FIELD IMPLEMENTATION

The objectives of this thesis discussed in Section 1.3, are associated with a recent study at the University of South Carolina that focused on the implementation and validation of a StereoDIC equipped Unmanned Aerial Vehicle (UAV) through field testing in outdoor settings with the initial implementation and field testing applied on railroad bridges. This chapter presents the study on the development and application of the speckle pattern for the StereoDIC-UAV in view of the challenges posed by the field implementation of the airborne StereoDIC in railroad bridge monitoring. The following sections discuss first the site selection and introduce the UAV system. Subsequently, a detailed discussion on the speckle development and application is presented.

4.1 Site Selection

The railroad bridge site for the field implementation was selected from the bridge inventory of CSX within proximity to the University of South Carolina laboratories. The selection criteria are governed by the need for unobstructed air space that will not require any traffic control, or any non-standard safety measures for the deployment of the UAV. The selected bridge site is in the CSX Hamlet subdivision over Park Street and is shown in Figure 4.1. The bridge is a five-span steel bridge and the first span off Park Street was selected for the field testing. The bottom of the girder is 16-feet above ground level and is easily accessible by boom lift.

(a)

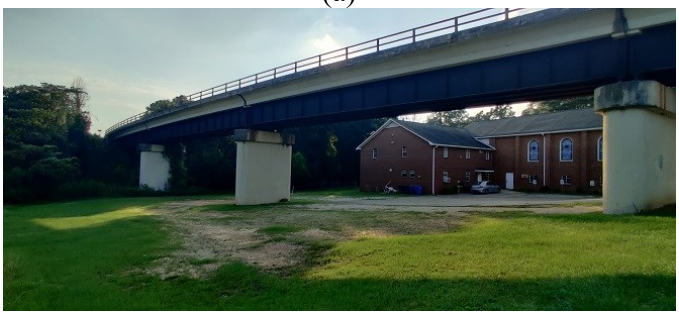

(b)

Figure 4.1 Park St. Bridge (a) West Facing Side [Field Side] (b) East Facing Side [Church Side]

4.2 Drone System

A UAS-system developed by the Unmanned Systems & Robotics Lab (USRL) at the University of South Carolina was used for data acquisition at the site [63]. The specifications of the system are in Table 4.1. The platform is commercially available and customizable. The onboard computer was used for both the DIC system and flights. The StereoDIC is of interest to this research, specifically the resolution of the cameras and existence of onboard lights.

4.3 Speckle Characteristics

Three bridge panels were captured during acquisition, and this resulted in a desired width of the field of view to be 11.81 feet [63]. In view of the DIC camera system and the field of view, the UAV needs to fly 4 meters away from the panels. At this distance, the cameras were able to capture a field of view of width 4.48 m and height of 2.36 m.

Table 4.1 UAV System Specifications

	Parameter	
UAS Platform	Platform	Aurelia X6 Standard Long Endurance UAS
	Max Payload	5 kg
	Max Flight Time	45 minutes
	FCU	CubePilot Blue
Onboarding Computing Power	Computer	Intel Nuc
	Processor	Intel i5 (4 x 2.3 GHz)
	RAM	32 GB
	Storage	1.5 TB
StereoDIC	Resolution	4096 x 2160
	Frame Rate	42 fps
	Lens	Adjustable focus and aperture; 12 mm
	Onboard Light	20 W LED light
	Synchronization	Hardware

Using the equations discussed in Section 3.1.3, the minimum speckle size was determined.

$$resolution = 4026 \times 2160$$

$$field\ of\ view = 4.48 \times 2.36\ (m)$$

$$per\ pixel = \ 0.0011\ x\ 0.0011\ (m)$$

Since speckle should be 3 x 3 pixels, the minimum speckle diameter is 3.3 mm. However, a diameter of 5 mm was chosen to accommodate expected motion. The adequacy of the minimum determined size of the speckle was verified and validated in the laboratory.

4.4 Speckle Application

This section describes the speckle application as implemented in the field. The surface preparation is discussed first, followed by a discussion of the techniques for creating the contrast and for applying the speckle.

4.4.1 Preparation of Surface

The first fundamental requirement for a successful implementation of the DIC technology is that the speckle must adhere firmly to the surface where measurements are to be acquired. Consequently, the surface needs to be free of any debris, oils, and contaminants. The girders, on the other hand, are made of weathering steel, and as such, a thin layer of rust is present on the steel surface. It is necessary, therefore, to remove any loose rust material from the girder surface, in addition to any other debris and contaminants. Cleaning was achieved using a handheld wire brush for a light brushing followed by a wipe-down with a cloth. Although this is a relatively labor-intensive operation it is preferred to resource-intensive alternatives such as high-speed air blower, or chemical treatment that may also cause damage to the base material. A comparison of the scrubbed and non-scrubbed specimen surface is seen in Figure 4.2.

Figure 4.2 Comparison of Scrubbed and Non-Scrubbed Surface

4.4.2 Creating the Contrast

The second fundamental requirement for a successful implementation of the DIC technology, as discussed in Section 2.4.2, calls for local variations in contrast between the speckle and the background in all images. The weathering steel used in the bridge girders have a distinct dark brown color that is deemed sufficient to develop the necessary contrast with a bright white speckle. Consequently, it was decided to apply a bright white speckle directly on untreated steel plate surfaces. However, after the direct application of the speckle, the desired contrast was not developed, and it was necessary to create a white background for a black speckle application.

The conventional method of applying the background has typically been weather and rust resistant spray paint. A thin, but opaque, layer with little additional texture is obtained by spraying from an approximate distance of 12 inches from the surface always in the same direction. Generally, this paint dries relatively quickly but is important to maintain a thin and uniform layer. There are potential problems with opacity and thickness variation when larger areas are sprayed, and especially when wind speed increases. However, this method is a viable choice for background application due to the drying speed as long as certain requirements are met. Figure 4.3 below shows the use of spray paint for the application of a white background at the Park St. Bridge. Due to the altitude and subsequent wind as well as the large surface area, an inconsistent/splotchy background resulted. This can potentially interfere with the validity of results depending on the acquired data and relevant processing. The following images depict the application of the spray paint background as well as the result.

(a)

(b)

Figure 4.3 White Spray Paint Background (a) Applying White Background with Spray Paint (b) Resulting Background using White Spray Paint

To overcome the shortcomings of using spray paint, flat white exterior paint that is compatible with the relevant surface and is "durable" was used to achieve a quality background. By durable, it means that the paint is both weather and rust resistant and as well as suited to any potentially dramatic thermal variations. Valspar Storm Coat Exterior Paint in flat white was used and applied by roller and brushes. When using this type of paint, it can be more difficult to prevent lines and drips throughout the applied area due to a thicker consistency and switch to application via paint roller. The quality of the

background when the paint was applied via brush was compared to that via standard paint roller to determine the preferred method for use in the field. While the brush required fewer layers, there were increased irregularities such as streaks and drips. This made the roller, which required more layers but applied more evenly, the more viable option for quality results. Also, when in the field, brushes are limited by the researchers' reach while most standard rollers can be attached to extendable handles. Therefore, a standard paint roller is the optimal method to apply a painted background to relevant areas of interest, especially when spray paint is not a viable option.

4.4.3 Speckle-by-Speckle Application

This speckle-by-speckle application discussed in section 3.4.5 technique applies the speckle one speckle at a time by tapping a single tip applicator on the surface leaving an imprint. The size of the speckle is controlled by the tip size of the applicator and the application pressure. Permanent ink pens (Sharpies), sponge tipped brushes, wood dowels and rubber tips were considered predominantly in a laboratory environment and with relatively small surfaces during our investigations to verify speckle size, contrast, paints, applicator materials, and to test the desired surface preparation before speckling. Figure 4.4 depicts the resulting speckles. While Figure 4.4(d) shows a fairly consistent density of the speckles, achieving the optimum density depends on the experience of the technician. It was also confirmed that while the dowel allowed good control, the ink was not applied evenly throughout a dot due to the porosity. This can be better seen in Figure 4.4(e). The use of permanent ink pens produced the best quality speckle.

(a)

(b)

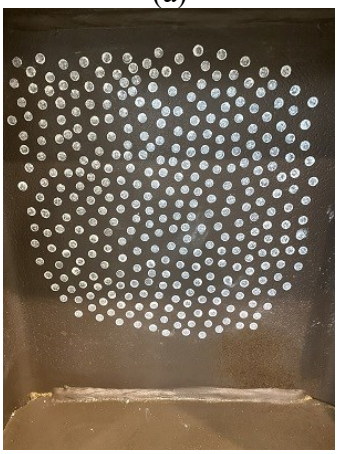

(c)

(d)

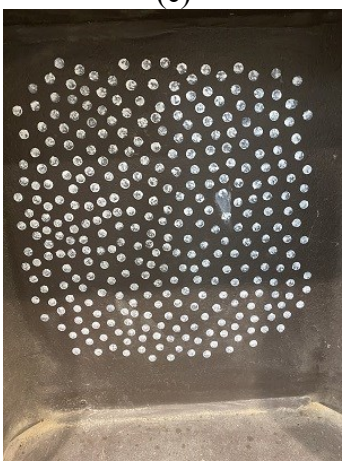

(e)

Figure 4.4 Speckle-by-Speckle Application (a) Speckle-by-Speckle Application on Support 1 (b) Speckle-by-Speckle Application on Support 2 (c) 3 mm Speckle-by-Speckle Application using Wooden Dowel (d) 3 mm Speckle-by-Speckle Application using Wooden Dowel [Zoomed] (e) 3 mm Speckle-by-Speckle Application using Rubber Eraser

The speckle-by-speckle application is extremely time-intensive, and the speckle quality, randomness and size depends largely on the experience of the operator and is not appropriate as the primary application method in the field. However, it was used for localized spot speckling to correct the speckle and improve its quality.

4.4.4 Application by Roller and Rocker Stamp

An alternative to the speckle-by-speckle application is the use of roller or rocker stamps discussed in section. In the present work, a roller stamp is selected since it increases coverage and speed in speckling the larger, flat surfaces. The rubber stamp carrying a random speckle of the desired diameter of 5 mm is wrapped on a roller. The roller was used in two field tests. In the first case, white-ink speckles are applied directly on the weathered steel web panel. Figure 4.5(a) shows the resulting speckle when white ink is applied directly on the surface of the weathered steel panel in the laboratory. There are some visible irregularities in the opacity of individual speckles, however, a satisfactory contrast was achieved. In the second case, black-ink speckles are rolled on a pre-treated web panel with a white background. In this case, blemishes may be caused by the roller slipping on the surface that now has a smoother texture due to the application of the white background.

In early experiments, both white-on-steel and black-on-white speckles were applied on the surface of the web panels of the Park St. Bridge. In the case of white-on-steel speckle it became progressively more difficult to successfully transfer the white ink from the roller to the surface. It is theorized that there was potentially a substance on the steel that interfered with the adherence of the ink and the substance was transferred on the roller, defacing the pattern on the stamp. The more often the roller was used, the worse the problem became. Figure 4.5(b) shows two panels covered in white speckle from the use of

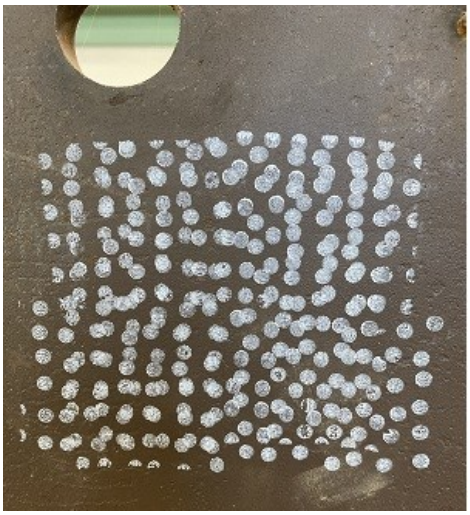

(a)

(b)

(c)

(d)

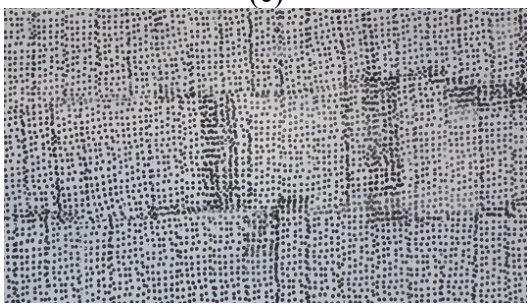

(e)

Figure 4.5 Speckle Application with Roller (a) White Speckle Applied with Roller in Lab on Support 1 (b) White Speckle Applied with Roller in Field (c) Applying Black Speckle with Roller in Field (d) Black Speckle Applied with Roller in Field (e) Inconsistencies in Black Speckle Applied with Roller in Field

a roller. The left panel was completed first with two passes over the area while the panel on the right was done last and only has one layer due to the progressive transfer problem. In addition, due to the windy and slightly cooler environment when working on the bridge's panels, the white ink dried rapidly whenever it was exposed, whether in the pad or on the roller clogging the roller and the stamp. This was not the case when using black ink, so it is possible that the differences in formulation of the separate colors was the cause. Figure 4.5(c) shows the black speckle applied via roller onto a white painted background and even at a distance, the high contrast is apparent. Figure 4.5(d) shows the resulting speckle as well as potential problem areas. Figure 4.5(e) shows where overlapping with the roller caused blending of the speckle imprints significantly affecting the speckle density and the dark-to-white balance. Thus, these areas are not ideal for digital image correlation analysis. Based on problems with contrast and transfer, especially in comparison to the black ink, the use of white ink in the field was discontinued for the Park St. Bridge project and it was not deemed ideal for this application. The white ink could, however, still potentially be viable for use in handheld printers, which will be discussed in a later section.

4.4.5 Self-Adhesive Sheets

As an alternative to the manual application of the speckle described above, a computer-generated speckle with the desired characteristics discussed in section 4.3 is pre-printed on self-adhesive sheets and subsequently applied to the surface of the girder web. The speckle pattern is laser-printed onto matte self-adhesive synthetic sheets. The application was much faster than the roller stamp, requires pretreatment of the surface but does not require a white painted background. Although the method produced a consistently high-quality speckle, it is not free of shortcomings. Transferring the sheets on the web

surface needs to be achieved in a way that eliminates, or at least minimizes, formation of air pockets and creases. The effects of trapped air on the adherence of the speckled sheets on the specimen surface are pronounced when changes in temperature cause the expansion and contraction of the trapped air. The speckled, self-adhesive sheets adhered firmly on the pre-treated steel surfaces. However, when applied on concrete surfaces, consistent problems with the adhesion were observed. This has led to the conclusion that the self-adhesive sheet method is only suitable for specific surfaces such as weathered steel. Figure 4.6(a) shows the speckled shelf-adhesive sheets being applied to the bridge surface. When applying the sheets, it was best to wear gloves to prevent natural oils on skin from interfering with the adhering capabilities or matte level of the paper. Each sheet was applied slowly with light pressure to force out as much air as possible during the application process. To the naked eye, this seemed to be successful but, the accuracy from measurements is unconfirmed. Figure 4.6(b) shows the pattern as well as the edges that result from aligning the sheets. After discussion, it was determined that these edges were not detrimental to the data processing. Although a high-quality speckle with firm adherence is attained immediately after application, there are concerns with the durability of the adhesion for long term monitoring, since there was evidence of adherence loss at the sheet edges within three months after first installation and exposure to the elements. During a later site visit, Figure 4.6(c) shows some limited lifting at the edges of the panel was observed, but overall, the sheets held well.

(a)

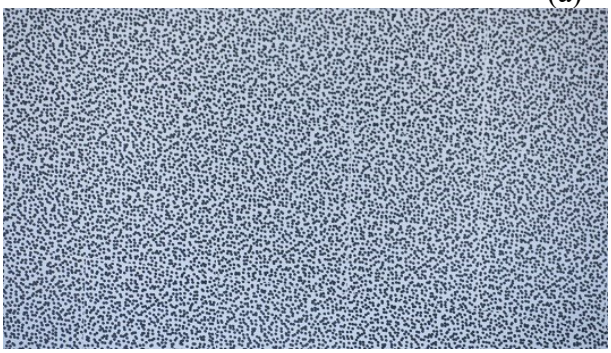

(b)

(c)

Figure 4.6 Self-Adhesive Sheets in the Field (a) Applying Self-Adhesive Sheets in the Field (b) Self-Adhesive Sheets Speckle after Application (c) Self-Adhesive Sheets after Weeks on the Bridge

4.4.6 Handheld Printer

As the need for more precise speckle application methods became apparent along with the unproven nature of the speckle self-adhesive sheets, handheld printers were introduced to factor out some of the human and mechanical errors present with roller and/or stamp applicators. These printers are available in various models of varying quality and capability. Most of them can print in either black or white, although interchangeability of ink is not guaranteed depending on the model. This means that the printers can apply speckle in black or white ink, but some models require the purchase of an entirely new printer to change the ink color. The printers are capable of printing long distances in one

movement and creating high and variable contrast depending on the uploaded file. The file along with the printer and ink used and the operator's ability directly dictate the quality of the speckle and thus quality of the data. Furthermore, generally, both the printer and the ink are expensive so covering large areas can have a significant cost.

The speckle pattern itself is designed using Correlated Solutions' "Speckle Pattern Generator" software where the user can select the diameter and density of the pattern. This is then converted to a bitmap or pdf based on the researcher's preference then uploaded to the printer using a flash drive. Once the files are visible on the printer's screen, they can be saved directly to the printer's system so the flash drive is no longer necessary, and the same files can be accessed repeatedly.

4.4.6.1 Printer Specifications

The printers used in the field tests and experiments and their specifications are shown in the images and tables below. The first printer purchased was the SNEED-Jet Freedom Handheld printer from SNEED Coding Solutions, Inc [64] seen in Figure 4.7(a). This printer is able to print one to eight lines of text with a height range of 1 mm to 25.4 mm (0.04 in to 1 in) on a multitude of materials including aluminum, cardboard, glass, paper, plastic, metal, etc. It is capable of printing with a 300-dpi resolution which is the optimal resolution for the speckle pattern. It has a rechargeable battery with about 7 hours of life before needing to be recharged. It runs on a Linux system and has a TIJ Thermal InkJet nozzle. Once the printer is used for a certain ink color, it cannot be interchanged. Therefore, if it is being used for black speckle, a separate printer must be used for white speckle. While this printer is capable of producing quality speckle, it was recognized that using it to speckle the relatively much larger panels of the bridge would require an

extensive amount of time so other printers were investigated. One such printer was the Bentsai B85 Handheld printer [65], which is pictured in Figure 4.7(b). This printer has a maximum printable height of 100 mm (4 in) using four individual, staggered ink heads that are 25.4 mm (1 in) each, as seen in Figure 4.7(c). This printer can also print a maximum length of nine feet on both non-porous and absorbent surfaces. Furthermore, unlike the SNEED-Jet printer, different ink types can be interchanged within the same printer.

(a) (b) (c)

Figure 4.7 Handheld Printers (a) SNEED-Jet Freedom Handheld Printer [1-inch print height] (b) Bentsai B85 Handheld Printer [4-inch print height] (c) Bentsai B85 Handheld Printer Ink Heads

4.4.6.2 Speckle Printing

The first time the printers were used in the field, the surface was prepared and painted white using Valspar Exterior Storm Coat Paint in Flat White. Once the paint was dry, two researchers went up in the boom with both the InkJet and Bentsai printers as well as a chalk string line. This was used to mark a straight line for the first pass with the printers. The following passes were based off the previous one. White out was used to mark on the side of the printers where the ink heads were to best estimate the location being printed. Using the uploaded speckle pattern, the Bentsai printer was used to print the majority of the panel with the InkJet filling in gaps. These “gaps” arose when the print was ended before the end of the uploaded pattern since the print heads were staggered, so was the end

of the stroke. Then, the beginning of the continued print is also staggered. To try to avoid large gaps from the system delay, there was a purposeful overlap between “sets”. This delay was caused by the time it took for the encoder to register and communicate movement and location. Figure 4.8(a) shows the gaps and overlaps that can occur.

Similar problems can also arise if the placement of the printer is misjudged and a thin gap between the lines can occur. When this happened, the one-inch Inkjet printer was used to fill in the blank spaces left behind, as pictured below in Figure 4.8(b). However, this caused problems with the contrast as many of the overlapped areas were too dark and the speckle had merged, interfering with the DIC processing.

(a) (b)

Figure 4.8 Problems in Printing (a) Problems with Initial Printing Method [overlaps and poor contrast circles] (b) Overlaps and Staggered End of Print

The second time in the field with the printers, paper and painters’ tape was used to prevent the staggering and the overlap between the printed sections, respectively. This was done by printing the first line according to the chalk line guide until just before it became out of reach from within the boom, placing a piece of paper where the print is to end and continuing the print until completely on the paper to create a complete vertical line and avoid the staggering. Then, the print was canceled and restarted to prevent the stagger at the beginning of the section and each ink cartridge head was wiped with a lint-free

microfiber towel to prevent streaking while tape was laid along the edge of previous line to prevent overlap of the prints. Figure 4.9(a) shows this in action in a laboratory environment on a piece of plywood. Once the efficacy was proved in the lab, the taping method was implemented in the field, as seen in Figure 4.9(b). For efficiency, one person in the boom ran the printer and canceled and restarted prints while the other held the papers and taped the lines. It was better to have someone holding the paper rather than taping it to the panel because the wind caused a need for a lot of tape, and it was very time consuming. Therefore, the paper being held and quickly moved was the preferred choice.

(a) (b)

Figure 4.9 Using Painters' Tape (a) Use of Painters' Tape in Lab (b) Use of Painters' Tape in Field

4.4.6.3 Speckle Correction

Mistakes and problems are inherent to the research process. As previously discussed, after the first field visit, it was recognized that the speckle patchwork and fixes would be necessary for optimal data acquisition and processing. As such, there was a need to develop a way to fix the spots that had problems which was first practiced in the lab then implemented in the field. The method followed the steps listed below:

1. Identify problem areas within the speckle either using the naked eye or during the StereoDIC image processing. Most problematic sections can be seen without cameras or software as experience with how the speckle should looks and what the data processing requires is gained.
2. Tape borders around area using painters' tape to prevent the paint from covering "good" speckle which would increase required time and work.
3. Paint over existing speckle with the same paint (color and brand) that was used for the original background. If the original paint is unavailable, the closest match possible can be sufficient but must be considered when looking at the data and results.
4. Reprint the speckle over the new background, using papers and the tape to prevent overlap between the old and new speckle. In locations where there were misprints due to surface irregularities, the speckle may need to be applied manually because the encoder on the printers have trouble.

This method was first implemented in the field where it was realized that the method needed to be refined to maximize efficiency. Therefore, it was brought to a laboratory environment where a piece of plywood was speckled. The surface had a multitude of divots and deformities which allowed for correlation between them and the speckling process. Figure 4.10(a-b) depicts the first round of speckling done in the lab with the painters' tape applied to border the problem areas as well as a closer photo of the divots that caused problems. The taped areas were then painted over according to step three, an image of which can be seen in Figure 4.10(c).

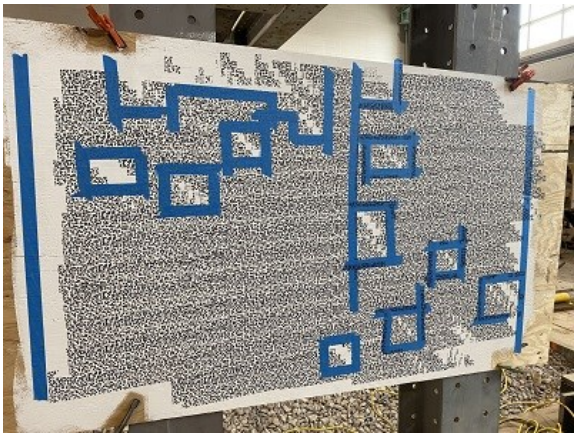

(a)

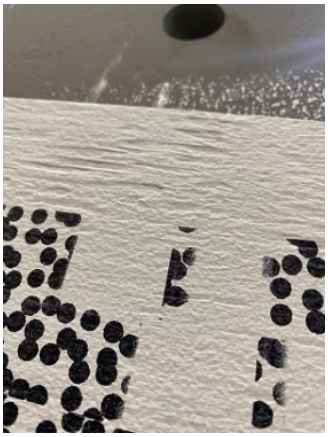

(b)

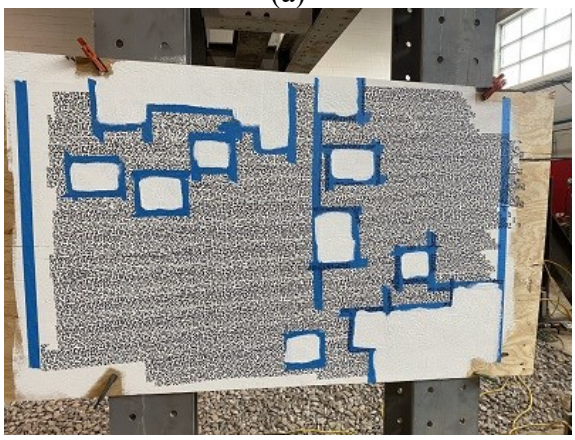

(c)

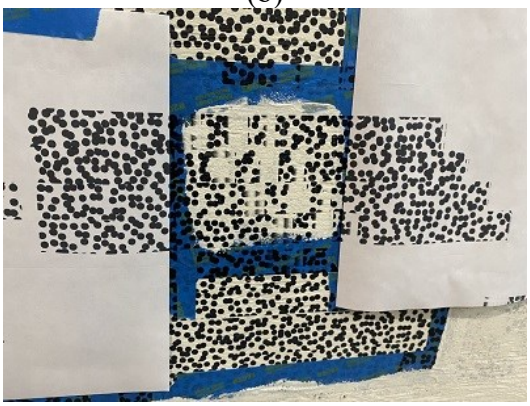

(d)

Figure 4.10 Practicing Speckle Correction in the Lab (a) Patching Practice in the Lab [Taping Stage] (b) Rivets in Plywood and Resulting Printing Problems [circled] (c) Patching Practice in the Lab [Painting Stage] (d) Problems with Patching Practice [Reprinting Stage]

Re-speckling the problem areas was then attempted to confirm the cause of the misprints was the surface and not human error. When reprinting, there were still misprints which confirmed the theory of the ridges in the surface interfering with the encoder. This happens because the printer's encoder, which tracks the movement for accurate printing, briefly loses contact with the surface so the encoder stops recognizing the printer's movement. This means there are missed patches, as seen in Figure 4.10(d). This image also shows how paper was used to prevent overlap when re-speckling the section. There have not been problems with the ink bleeding the paper onto the surface under it. While in the lab, the timing for the work was tracked and has been summarized in Table 4.2.

Table 4.2 Procedure Timing in the Lab

Task	Time (min)	Notes
Painting panel / coat	6	Only 1 coat on plywood (usually two on steel)
Paint drying	28	Was very humid in lab without sun to assist with drying (unlike in the field)
Printing Speckle "Part 1"	20	Had to stop to change out ink cartridges
Changing Ink cartridge	6	Without needing to move boom
Printing Speckle "Part 2" and started taping patch areas	30	While one person speckled, the other was holding the paper and taping the problem areas to be patched.
Paint problem patches	14	Had to do multiple coats with a need for it to slightly dry in between
Paint drying and beginning clean up	34	
Print speckle on painted patches	22	A number of problems with printing on the plywood so a portion of time went to working with the printer and encoders to try to solve the problem
Total (Paint and Speckle)	90	
Total (Final Result)	160	

After gaining experience with the speckling method in the lab, it was brought back to the field. There, the previously speckled panels were completely repainted, except for the one with the self-adhesive sheets. Once the paint was applied and dry, the speckle pattern was printed onto the panel using the paper and painters' tape to prevent overlaps. This is seen in Figure 4.9(b).

Regarding mistakes, the patching method was used where appropriate, shown in Figure 4.11. However, there were some areas where concave areas made it so that the printers' encoders did not pick up movement which resulted in repeated problems with

misprinting. In these situations, the sharpies were used to repair the pattern. While the sharpie speckle is distinguishable from the printed speckle, it is still acceptable. The timing in the field using the preferred procedural steps can be seen in Table 4.3.

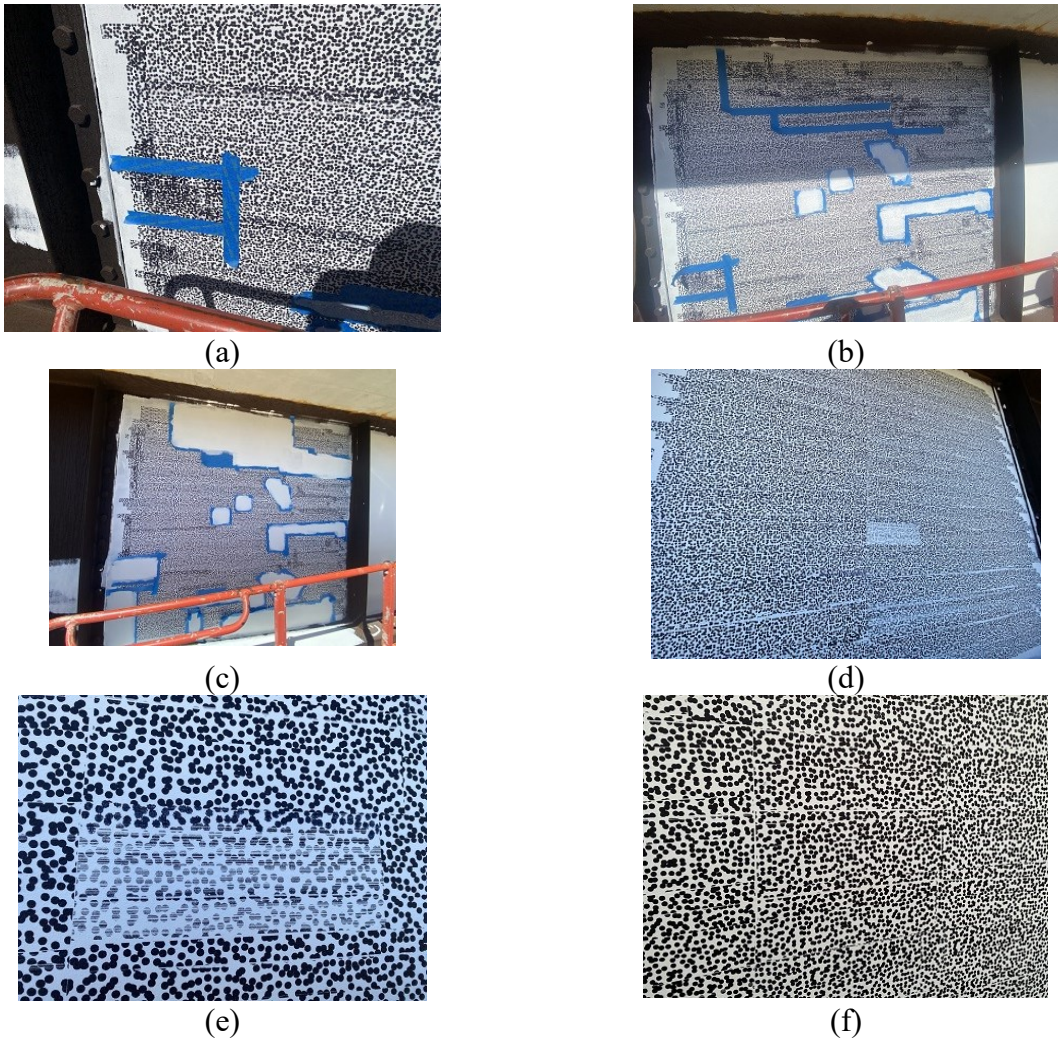

(a) (b) (c) (d) (e) (f)

Figure 4.11 Speckle Correction in the Field (a) Patching Area in Field [Taped] (b) Patching Larger Areas in Field [Taped and Painted] (c) Patching Larger Areas in Field [Painted] (d) Areas Requiring Sharpie to Fix due to Rivets (e) Patched Area Comparison [Before] (f) Patched Area Comparison [After]

Table 4.3 Procedure Timing in the Field

Task	Time (min)	Notes	Figure(s)
Arrival/Set Up	10	Unloading car, taking photos	4.12(a)
Start lift and get into place	15	Could not find key then stalled on incline	
Paint 1st panel (midspan, West facing side)	14		4.12(b)
Moved lift to pier	10		
Painted panels at pier	15	1 full panel and 2 small girder sections and 1 patch on a full panel Missed painting spot in corner due to wasp	4.12(c)
Moved lift to mid span East facing side	6		
Paint 2 of 3 mid span (East facing side) panels	14		4.12(d)
Moved lift for 3rd panel	5		
Paint 3rd panel	10		
Returned to ground, switched out supplies to speckle	27	Got water and snacks as well	
Moved lift into place for speckling field side mid span	5		
Speckle 1st panel mid span (West facing side)	75		
Moved to the pier	5		
Speckled small patch	15	Attempted to speckle all previously painted sections but the wasps were very aggressive and charged researchers within 3 feet of the nests (which were on the panels)	4.12(e) 4.12(f)
Moved to East facing side	21	Encountered problems with being on and incline where the lift automatically shuts down and prevents movement which prevents correction.	
Speckled 1st panel	57	Did not finish, stopped for lunch	4.12(g)

Task	Time (min)	Notes	Figure(s)
Returned to ground	3		
Started up again, moved lift into place	12		
Speckled one panel (second of three)	66	Returned to ground for break due to oil leak in the lift and mechanical needed to go up to pier	4.12(h)
Went up to pier	9		
Tried to speckle pier	24	Wasps were still a problem	
Moved back to East facing side	10		
Specked third and final panel (including sharpie fixes)	75		4.12(i)
Moved back to pier	12		
Speckled small girder sections of pier	31	Still couldn't speckle one of the big panels because of wasps	
Total	607	Lost a lot of time because of mechanical problems and wasps and were unable to complete as much as we would have liked	4.12(j) 4.12(k) 4.12(l)

(a)

(b)

(c)

(d)

(e)

(f)

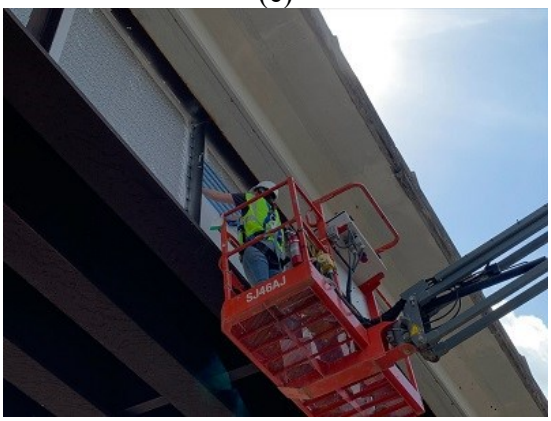

(g)

(h)

(i)

(j)

(k)

(l)

Figure 4.12 Full Procedure in the Field (a) Setting Up in Field (b) Painting Panel [Midspan West Facing Side] (c) Painting Panels [Pier] (d) Painting Two of Three Panels [Midspan East Facing Side] (e) Speckle Patch of Panel [Pier] (f) Speckling Panel with Wasps [Pier] (g) Speckle Panel [Midspan East Facing Side] (h) Speckling Two of Three Panels [Midspan East Facing Side] (i) Returned to Pier (j) Final Results [West Facing Side] (k) Final Results [West Facing Side Pier] (l) Final Result [East Facing Side]

As the speckle was evaluated, it was realized that the consistent use of the same bitmap, along with the method of restarting the print at the beginning of each line led to repetition within the pattern, as seen in Figure 4.13. While the pattern was still considered acceptable, the lack of randomness could lead to problems with pattern tracking and thus deformation and change detection of the member. Therefore, it was determined that a separate bitmap should be used for each line within the AOI.

Figure 4.13 Repetition within Printed Speckle

4.5 Data Acquisition

Throughout the various speckle application method iterations, the UAS was deployed to capture images to be processed to assess the quality of the pattern. During these flights, the system was remotely piloted by a person. However, once the speckle pattern was finalized, markers, seen in Figure 4.14(a), were placed to flag the area the system was to focus on. During deployments, the system was first operated by a human pilot until it was near the AOI, at which time the system could establish a visual tether and fly autonomously and hover in the desired position until the necessary images were

captured. Then, the human pilot regained control to land the system [63]. Figure 4.14(b) depicts the UAS flying while a train loaded the bridge.

(a)

(b)

(c)

Figure 4.14 Data Acquisition (a) Final Speckle with Visual Tether Markers for Autonomous Flying (b) Deployed UAV (c) UAV

Calibration was performed before and after each deployment and was used to verify that there was not a significant change in the relative position of the two cameras. A lack of significant change signified that the deployment did not impact the imaging system [63].

Deployments were performed on the unloaded bridge to obtain a reference point for the state of the bridge. When the bridge was loaded, deployments lasted from a few minutes before the train arrived at the bridges through as long as the power supply was able to support flight and acquisition while retaining enough power to land safely. Ideally, this lasted through the loading and for a few minutes after to obtain the unloaded reference, full loading sequence, and any transient response before the bridge returned to the default state [63].

4.6 Data Processing

For this project, VIC-3D was used for processing the acquired DIC images. Projects in this software must include speckle images (including at least one reference images), calibration, and one or more area(s) of interest [66]. A different calibration was performed for each field visit as well as in between each collection.

Once all images were saved and brought into the project file in VIC-3D, the calibration was performed with the necessary settings changed from the default. The main one was the calibration panel size, which was 12x9 – 70 mm.

Next, the AOI within the FOV of the footage was defined. Within this AOI, distinct features are selected to act as starting points within the AOI. This is also referred to as initial guess selection within VIC-3D software. Generally, this is necessary in cases such as the following [66]:

- Multiple, large camera angles (rather than a single stereo angle)
- Highly curved surfaces such as cylinders
- Large rotations between successive images
- Very fine or indistinct speckle patterns
- Poor calibration

However, in the case of this project, it was to compensate for movement of the drone between images which could "confuse" the software with jumps between locations. This made it easier for the software to correlate images based on the same, easily identifiable point and calculate the strain and deformations from there. It also has the added benefit of typically increasing the analysis time.

The user parameters and settings were not changed from the default values as the software was able to recommend the optimal ones. The subset was 49 x 49 pixels, and the step size was 7 pixels [63]. From there, the images were processed to produce the relevant data. However, there were still effects from rigid body motion that needed to be accounted for. This was done through average transformation, which is also done through VIC-3D.

CHAPTER 5

GENERAL DISCUSSION AND RECOMMENDATION

5.1 Summary of Implementation

No matter the chosen method of creating a solid background and speckle, the general procedure and needed materials in the field remain the same. There are several necessary materials for successful application and analysis. Access to the members is imperative, whether it is through a lift or access from the deck. When necessary, choosing which lift to rent/buy/use has both basic and more unknown criteria. It must be able to reach the top of the area of interest and have a basket that fits at least two people and any equipment. Also, a wide reach with minimal adjustments on the ground and a basket that can swivel from side to side is extremely useful, especially in hard to access/maneuver areas. This includes uneven/inclined terrain, restricted access, piers, and more. Figure 5.1 depicts the lift used for the Park St. Bridge.

Figure 5.1 Park St. Bridge Lift

Personal protective equipment (PPE) is needed for all fieldwork and includes the basic items such as hard hats, reflective vests, eyeglasses, gloves, and steel toed boots. So a lift is being used, harnesses are also necessary; two people working in tandem is best so a minimum of two to three harnesses is preferred. Three is preferred so that if one person leaves or takes a break, the harnesses do not need to be constantly resized which can take a relatively significant amount of time. Table 4.1 depicts which materials are applicable to each method of application and Table 5.2 denotes a summary of these materials.

Table 5.1 Required Materials by Application Method

Materials List	**Application Method**				
	Speckle-by-Speckle	White Roller	Black Roller	Self-Adhesive Sheets	Printers
Prep Work	X	X	X	X	X
Resources to Access Site	X	X	X	X	X
Paint and Related Materials for background Contrast	X*		X		X
Single Speckle/Roller/Printer Applicator	X	X	X		X
Ink and Ink Pad	X	X	X		
Guides		X	X		X
*Note: Necessary if a painted background is needed for background such as black ink on weathered steel.					

Table 5.2 Materials Summary

Item	Note
Access	Lifts, ladders, etc.
PPE	Including fall protection
Wire Brushes	To remove stuck debris on the surface.
Microfiber Rags	To remove debris from the surface and wipe ink heads of printers (if applicable)
Paint and Related Materials	Paint, paint tray and stirrer, rollers, and extending handles are specific to the use of exterior paint for a solid background. This may instead only be spray paint or nothing (self-adhesive sheets)
Painter's Tape	Recommended to not use ultra-strength tape as it can remove paint when tape is taken off the surface. Minimum width of ½-inch Blue Painters tape used in this work allows for adequate space for printer overlap.
Single Speckle Applicator	Rubber-like material is recommended.
Ink and Ink Pad	Recommended ink is permanent, water and alcohol resistant, and appropriate for porous and non-porous surfaces.
Rollers	
Self-Adhesive Sheets	Standard self-adhesive paper is not appropriate. Recommended type is a printable vinyl sticker paper for laser printers with matte white waterproof finish. Standard letter size 8.5"x11" used in this work.
Printers and Related Materials	See Section 4.4.6
Acetone	To remove paint, ink, or adhesive when necessary. Usually, the adhesion of the self-adhesive sheets is not so strong as to require this for removal.
Notebook and Pen	For field notes
Miscellaneous Tools	General tools for any unforeseen issues. Includes hammer, tape measure, screwdriver, etc.

General Workflow: The general workflow steps are summarized below and the workflow is shown in Figure 5.2.

1. Access AOI
    a. If using a lift, make sure to consider the inclines of site and how to maximize the area of interest that can be reached
2. Prepare surface at areas of interest per Section 4.4.1
3. Paint areas of interest per Section 4.4.2
4. Speckle areas of interest per Sections 4.4.3, 4.4.4, 4.4.5, and 4.4.6
5. Retouch speckle with a sharpie (if necessary) per Section 4.4.6.3
6. Identify problem areas
7. Access problematic areas
    a. Reposition crew as necessary
8. Paint over problem areas to patch
9. Re-speckle (patch) problem areas per Section 4.4.6.3
10. Retouch speckle with sharpie (if necessary)
11. Check for any missed or new problematic areas and repeat Steps 6-10 if necessary
12. Prepare and calibrate UAS per Section 4.5
13. Fly UAS and acquire data per Section 4.5
14. Recalibrate UAS per Section 4.5
15. Download and process images/data per Section 4.6

*Note: Step 12 can be done in tandem with Steps 1-11.

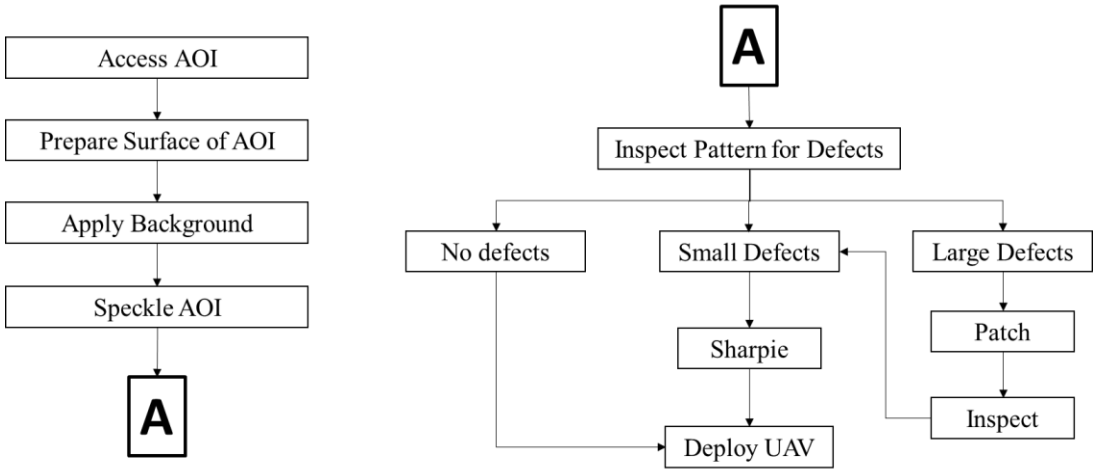

Figure 5.2 Workflow

5.2 Issues and Resolutions

The benefits and lessons learned for each method have been compiled into the following table to properly illustrate the comparison. This includes the benefits of each method as well as the relevant shortcomings/disadvantages. The speckle-by-speckle application method was very time consuming and dependent on the understanding and skill of the technician. The roller, when used with white ink on the clean surface, had the benefit of not needing to apply a painted background. However, there were consistent problems with adherence and contrast. The ink dried too quickly to properly transfer from the ink pad to the roller to the surface. The roller with black ink on a white painted background, the contrast and Ink adherence had significantly improved compared to the white ink. However, overlapping passes can cause problems with the drastically varied density. While not as time consuming as speckle-by-speckle application, the rollers are still relatively inefficient. The self-adhesive sheets were more efficient and always had a quality pattern, but the sheets had to be applied with precision to prevent entrapped air. This would disrupt adherence to the surface, especially as ambient temperature changed, and the trapped air

expanded and contracted. After time on the specimen, the adherence of the sheets to the surface was diminished and would require replacement. Handheld printers are an efficient and precise method but require effort to avoid gaps and overlaps. This could be accomplished through painters' tape and plain paper. Technicians must be aware of the ink and ink head status and wipe the ink heads between each pass to avoid smears and blocked cartridges. To avoid repetition within the pattern, a separate bitmap pattern is recommended for each pass. A summary of the benefits, shortcomings, and potential resolution is depicted in Table 5.3.

Table 5.3 Method Comparison Summary

Method	Benefits	Shortcomings	Resolutions
Speckle-by-Speckle Application	Inexpensive.	Labor intensive.	
Roller (White ink on Surface)	No need for background.	Ink adherence.	
	Less labor intensive than speckle-by-speckle	Poor Contrast.	
	Less expensive than handheld printers.	More expensive than speckle-by-speckle	
Roller (Black ink on white paint)	Better ink adherence and contrast.	Overlaps and gaps	Guides
	Less expensive than handheld printers.	Difficult to maintain speckle consistency	
Self-Adhesive Sheets	No background.	Entrapped air affects image-specimen correspondence (Section 3.1.1)	Thorough surface cleaning and meticulous application.
	Precise speckle.		
	Less labor intensive and expensive.	Durability of sheet adherence	
Handheld Printers	Precise speckle.	Expensive.	
	Less labor intensive.	Overlaps and gaps.	Guides.
		Repetition of pattern.	Different bitmaps per print.
		Wipe ink heads.	

5.3 Quality Evaluation

The speckle application methods discussed in this paper are varied in terms of both methodology and results. The performance of each method can be quantified via histograms which represent the gradation of black, white, and grays. It should generally

show an approximate 50/50 distribution of points between the black and white gray levels to signify quality contrast and density within the speckle pattern. This is shown by a bell-type curve with the two peaks as the “white” and “black” levels. Figure 5.3 from "Assessment of speckle-pattern quality in digital image correlation based on gray intensity and speckle morphology" depicts this concept [60]. In this figure, while each image shows acceptable histograms, (d) is the best. The large separation between the peaks means there are many gray levels between the lightest and darkest points, implying high contrast. The existence of peaks implies acceptable sharpness of the speckle.

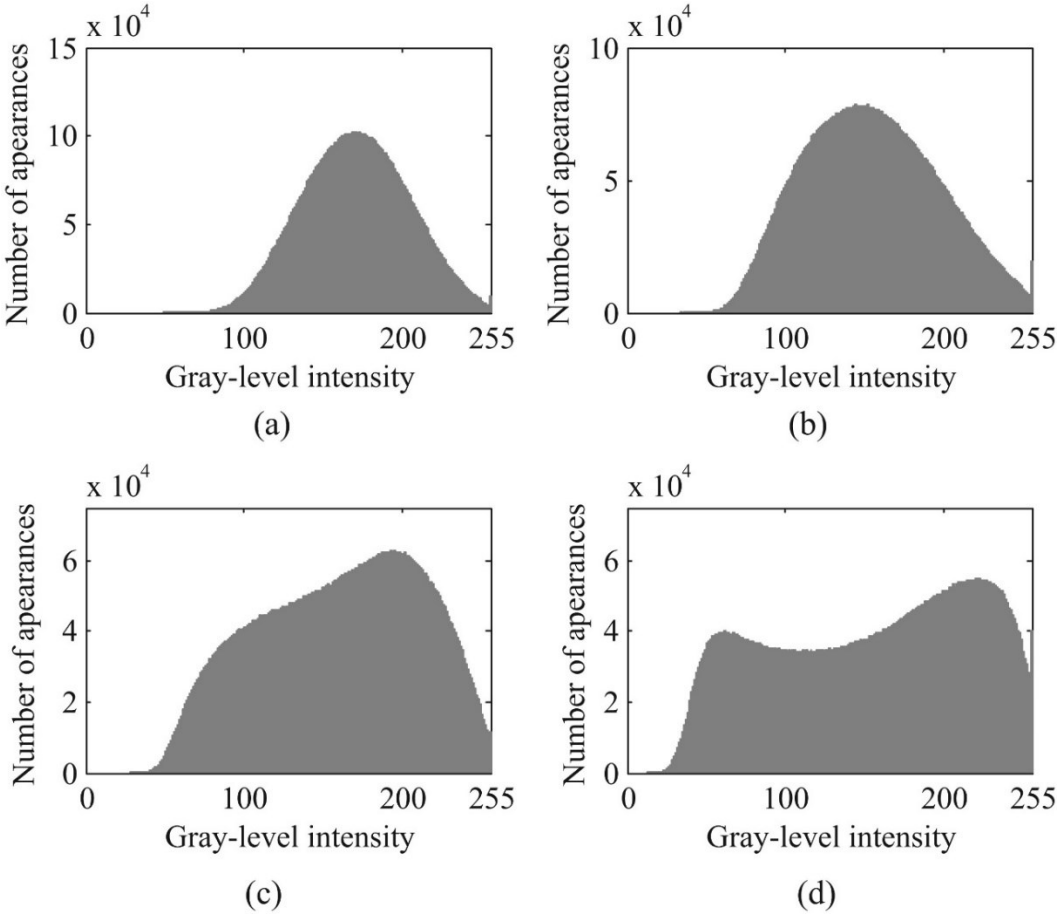

Figure 5.3 Sample Histograms

Histograms for each of the speckle methods used in the field have been developed to facilitate the comparison and analysis of the quality of the speckle patterns produced relative to their usefulness in DIC. The comparative histograms can be seen below in Figure 5.4. The black area is over the entire AOI of the panel while the blue, green, and red squares are smaller areas of analysis within the entire panel to compare the quality across the FOV. While each set of histograms show acceptable quality of the images, those produced by the self-adhesive sheets and the handheld printers are distinctly higher. This implies that the displacement and deformation measurements from the self-adhesive sheet and printed speckle would be of higher quality and accuracy. However, the durability of the adherence of the sheets could potentially diminish these results.

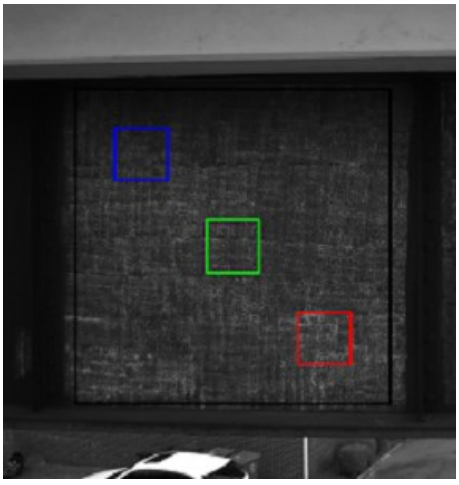

(a)

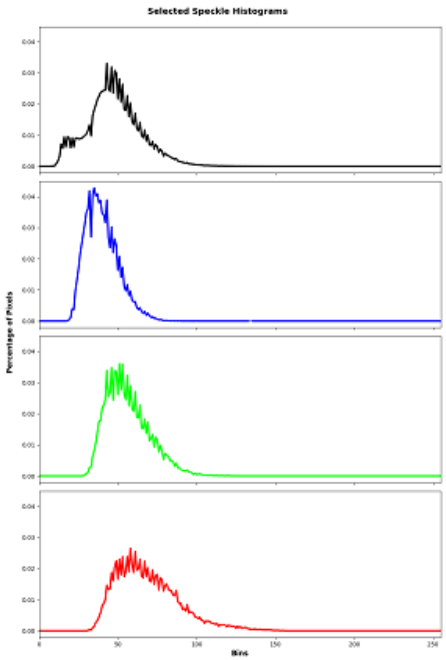

(b)

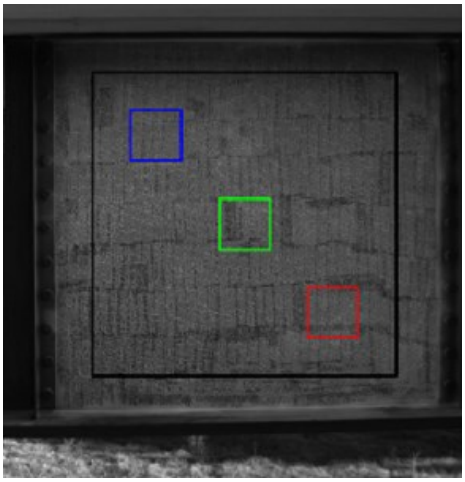

(c)

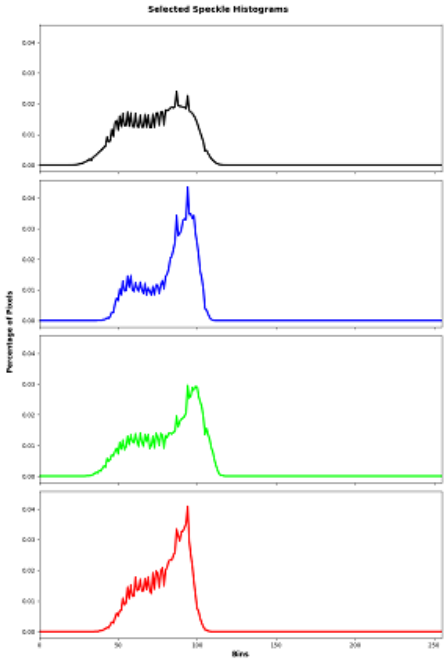
Selected Speckle Histograms
Percentage of Pixels
Bins

(d)

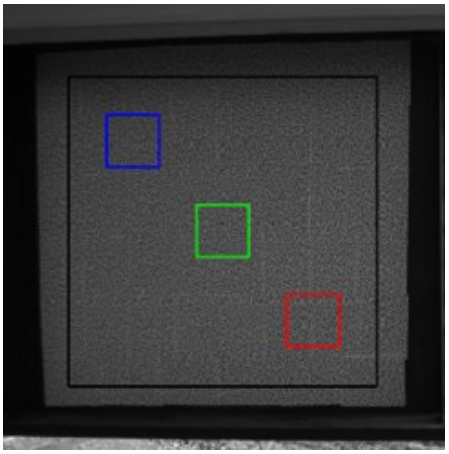

(e)

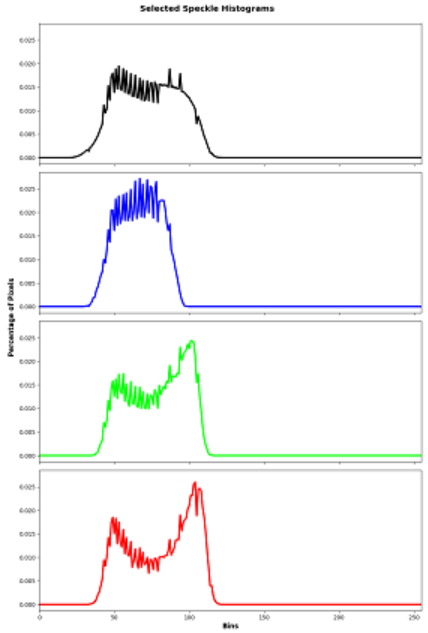
Selected Speckle Histograms
Percentage of Pixels
Bins

(f)

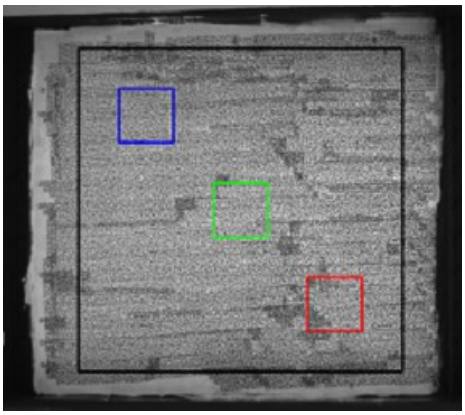

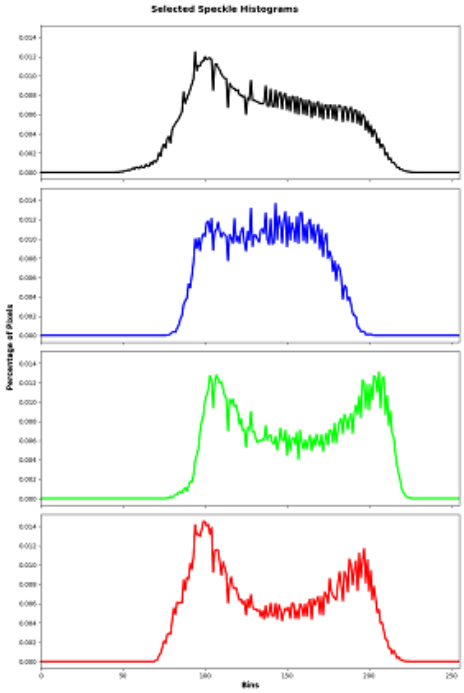

(g) (h)

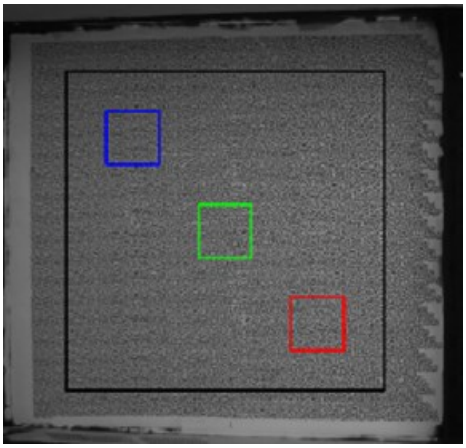

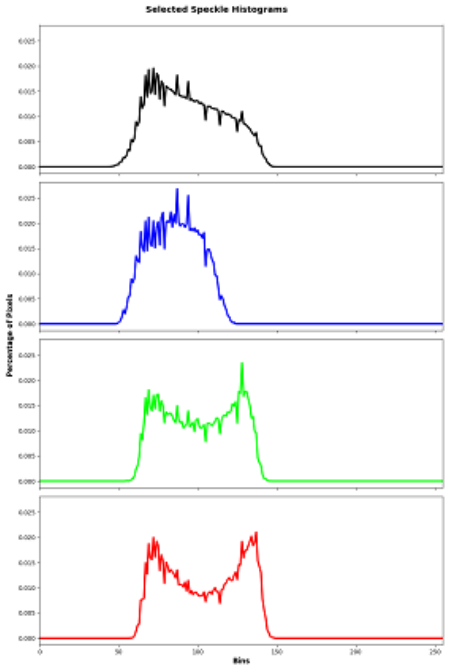

(i) (j)

Figure 5.4 Histograms of Speckle by Application Method (a) White Roller Speckle (b) White Roller Speckle Histogram (c) Black Roller Speckle (d) Black Roller Speckle Histogram (e) Self-Adhesive Sheet Speckle (f) Self-Adhesive Sheet Speckle Histogram (g) Printed Speckle [Without Taping] (h) Printed Speckle Histogram [Without Taping] (i) Printed Speckle [With Taping] (j) Printed Speckle Histogram [With Taping]

It can be seen, especially in Figure 5.4(g-j) that the quality of the speckle appears to improve when moving from left to right (blue to green to red). Because two panels were captured at a time, the center of the FOV was the joint of the panels, the edges are more out of focus. The progressive loss of focus as the AOI moves further from the center of the field of view is more clearly seen in Figure 5.5. Figure 5.5(a) shows the location of the smaller AOI across a panel while Figure 5.5(b) shows the varied focus in closer detail. It is reasonable to determine that this is the reason for the decreased quality between the red and green areas and the blue areas. This in turn negatively impacted the overall quality.

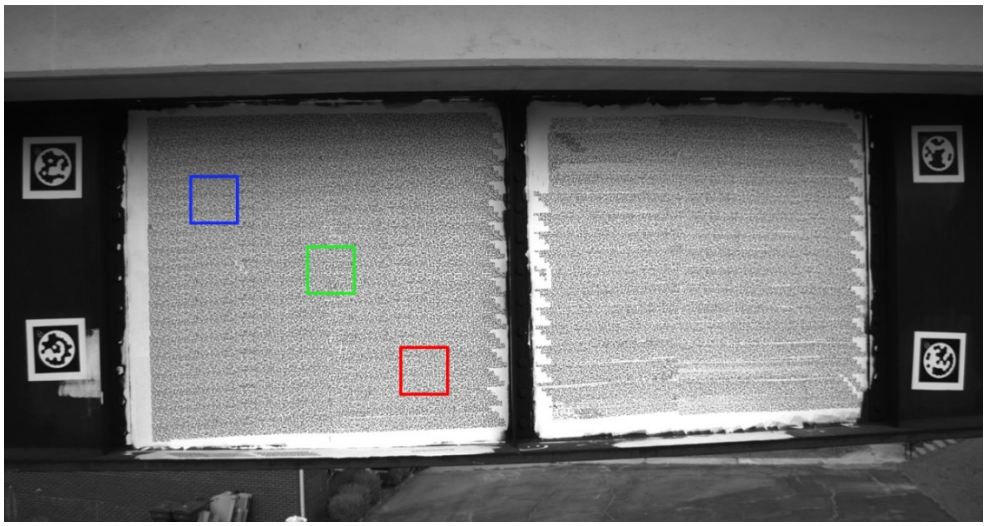

(a)

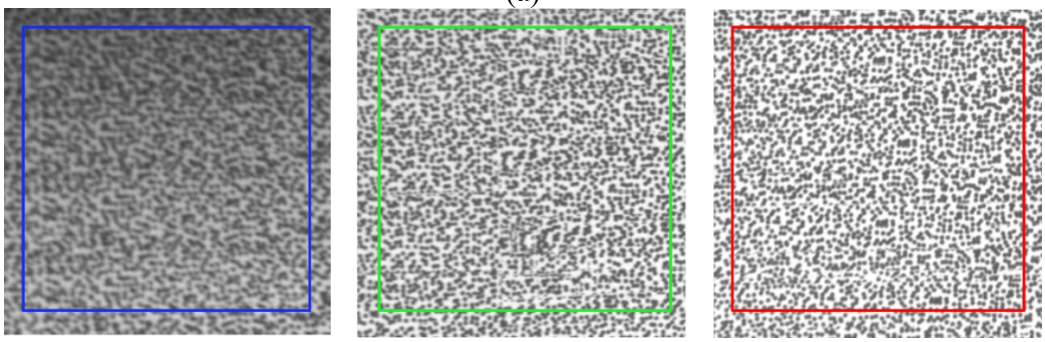

(b)

Figure 5.5 Focus Variation in Images (a) Field of View (b) Close-Up of Select Areas and the Loss in Focus

An overall comparative assessment of each methods is shown in Table 5.4.

Table 5.4 Comparative Assessment of Methods

Factors	**Method**				
	Speckle-by-Speckle	Roller with White Ink	Roller with Black Ink	Self-Adhesive Sheets	Handheld Printer (with guides)
Cost	Low	Medium	Medium	Low	High
Maintenance	Low	Low	Low	High	Low
Labor	High	Medium	Medium	Low	Low
Quality	Human dependent	Low	Medium	High	High
Time	High	Medium	Medium	Low	Low

5.4 Recommendations for Future Work

Future work is recommended to further optimize the procedure and methodology described. This includes work to determine if the self-adhesive sheets depict deformation of the surface with each speckle moving independently or if the whole sheet moves. An alternative to the self-adhesive sheets could be speckle pattern being printed on transfer paper to use on the surface. For handheld printers, white ink on a clean surface could be viable as it is a different ink than that of the roller, does not require slow-drying ink, and can print with consistent contrast.

CHAPTER 6

CONCLUSIONS

DIC is an imperative part of SHM methods for civil infrastructure and speckle is a key component of DIC data acquisition and processing. There has been research completed for the feasibility and implementation of stationary DIC systems but there is a lack of research into the feasibility of DIC-equipped UAV systems and the implementation of the necessary speckle pattern. Through the work detailed in this thesis, the optimized procedure and methodology for speckle application on large-scale specimens. This included iterative speckle application in the field with data gathered and processed for quality assessment of the pattern. It was determined that handheld printers used in tandem with guides and multiple bitmaps is the recommended method for large-scale applications. In all cases, surface preparation such as scrubbing is necessary.

Hand applying speckle is not desired because it is too time consuming with a high potential for mistakes. White ink on a roller, especially when directly applied on weathered steel, is impractical due to the comparatively poorer contrast and the problems with ink adhesion. White spray paint for background application is sufficient in controlled conditions such as that of a lab, but wind and large areas of interest keep it from being the optimal method. Black ink on a roller being applied on a white background has improved contrast but the variability in density and opaqueness can be detrimental. Flat white exterior paint applied with a roller is the preferred method for background application because it is

not affected by the site conditions such as wind and temperature. The color is also more consistent than that of the spray paint. The self-adhesive sheets are successful in providing sufficient contrast. However, the adhesion loses effectiveness after time on the surface, and it is unclear whether DIC will capture the deformation of the sheets, or the surface represented by the speckle. Printed speckle is optimal in terms of contrast and consistency. When guides such as painters' tape are used in the application process, the precision of the pattern is on par with the self-adhesive sheets without worries of adhesion. If the tape is not used and gaps and overlaps are allowed, the precision is closer to that of the black roller, but the consistency of the speckles are still better.

REFERENCES

[1] Minnesota Legislative Reference Library, Minnesota Legislature, 2022. [Online]. Available: https://www.lrl.mn.gov/guides/guides?issue=bridges#:~:text=Shortly%20after%206%20pm%20on,died%20and%20145%20were%20injured..

[2] B. Marr, "What is Industry 4.0? Here's a Super Easy Explanation for Anyone.," *Forbes Magazine,* 11 July 2019.

[3] S. Carroll, J. Satme, S. Alkharusi, N. Vitzilaios, A. Downey and D. Rizos, "Drone-Based Vibration Monitoring and Assessment of Structures," *Applied Sciences,* vol. 11, 2021.

[4] M. Kalaitzakis, N. Vitzilaios, D. Rizos and M. Sutton, "Drone-Based StereoDIC: System Development, Experimental Validation and Infrastructure Application," *Experimental Mechanics,* pp. 981-996, 2021.

[5] "Railroad Bridge Inspection Using Drone-Based Digital Image Correlation," FRA Office of Research, Development & Technology, 2022.

[6] S. Rehman and et al., "Nondestructive test methods for concrete bridges: a review," *Construction and Building Materials,* vol. 107, pp. 58-86, 2016.

[7] D. N. Farhey, "Bridge Instrumentation and Monitoring for Structural Diagnostics," *Structural Health Monitoring,* vol. 4, no. 4, pp. 301-318, 2005.

[8] S. Alampalli, D. M. Frangopol, J. Grimson, M. W. Halling, D. E. Kosnik, E. O. Lantsoght, D. Yang and Y. E. Zhou, "Bridge Load Testing: State-of-the-Practice," *Journal of Bridge Engineering,* vol. 26, 2021.

[9] C. Dong, S. Bas, M. Debees, N. Alver and F. N. Catbas, "Bridge Load Testing for Identifying Live Load Distribution, Load Rating, Serviceability and Dynamic Response," *Frontiers in Built Environment,* vol. 6, 2020.

[10] E. O. L. Lantsoght, C. van der Veen, A. de Boer and D. A. Hordijk, "State-of-the-art on load testing of concrete bridges," *Engineering Strutures,* vol. 150, pp. 231-241, 2017.

[11] Q. Han, J. Xu, A. Carpinteri and G. Lacidogna, "Localization of acoustic emission sources in structural health monitoring of masonry bridge," *Structural Control and Health Monitoring,* vol. 22, pp. 314-329, 2015.

[12] K. Ono, "Structural Health Monitoring of Large Structures Using Acoustic Emission-Case Histories," *Applied Sciences,* vol. 9, 2019.

[13] D. Tonelli, M. Luchetta, F. Rossi, P. Migliorino and D. Zonta, "Structural Health Monitoring Based on Acoustic Emissions: Validation on a Prestressed Concrete Bridge Tested to Failure," *Sensors,* vol. 20, 2020.

[14] R. V. Sagar and M. Butta, "Combined usage of acoustic emission technique and ultrasonic pulse velocity test to study crack classification in reinforced concrete structures," *Nondestructive Testing and Evaluation,* vol. 36, no. 1, pp. 62-96, 2021.

[15] D. Kang and Y.-J. Cha, "Autonomous UAVs for Structural Health Monitoring Using Deep Learning and an Ultrasonic Beacon System with Geo-Tagging," *Computer-Aided Civil and Infrastructure Engineering,* vol. 33, pp. 885-902, 2018.

[16] G. Karaiskos, A. Deraemaeker, D. G. Aggelis and D. V. Hemelrijck, "Monitoring of concrete structures using ultrasonic pulse velocity method," *Smart Materials and Structures,* vol. 24, 2015.

[17] Chencho, J. Li, H. Hao, R. Wang and L. Li, "Structural damage quantification using ensemble-based extremely randomised trees and impulse response functions," *Structural Control Health Monitoring,* vol. 29, 2022.

[18] A. C. Neves, L. Gonzalez, J. Leander and R. Karoumi, "Structural health monitoring of bridges: a model-free ANN-based approach to damage detection," *Journal of Civil Structural Health Monitoring,* vol. 7, pp. 689-702, 2017.

[19] W. Chiu and D. Barke, "Structural Health Monitoring in the Railway Industry: A Review," *Structural Health Monitoring,* vol. 4, no. 1, pp. 0081-0093, 2005.

[20] M. A. Barrera, "Railcar Wheel Impact Detection Utilizing Vibration-Based Wireless Onboard Condition Monitoring Modules," 2022.

[21] W. Zhai, Z. Han, Z. Chen, L. Ling and S. Zhu, "Train-track-bridge dynamic interaction: a state-of-the-art-review," *Vehicle System Dynamics,* vol. 57, no. 7, pp. 984-1027, 2019.

[22] S. Dabous and S. Feroz, "Condition monitoring of bridges with non-contact testing technologies," *Automation in Construction,* vol. 116, 2020.

[23] J. Kwiatkowski, W. Anigacz and D. Beben, "Comparison of Non-Destructive Techniques for Techlogical Bridge Deflection Testing," *Materials,* vol. 13, p. 1908, 2020.

[24] M. Iadicola and E. Jones, Eds., *A Good Practices Guide for Digital Image Correlation,* International Digital Image Correlation Society, 2018.

[25] E. Y.-H. Chao, "Development of a First-Generation Prototype Laboratory System for Rail Neutral Temperature Measurements," Master's of Science in Engineering, Department of Civil and Environmental Engineering, University of South Carolina, Columbia, South Carolina, 2022.

[26] M. Sutton, F. Matta, D. Rizos, R. Ghorbani, S. Rajan, D. Mollenhauer, H. Schreier and A. Lasprilla, "Recent Progress in Digital Image Correlation: Background and Developments since the 2013 W M Murray Lecture," *Experimental Mechanics,* no. 57, pp. 1-30, 2017.

[27] G. L. Hobrough, "The Photogrammetric Record," vol. 18, pp. 337-340, 2003.

[28] W. Peters and W. Ranson, "Digital imaging techniques in experimental stress analysis," *Optical Engineering,* vol. 21, no. 3, pp. 427-431, 1982.

[29] W. I. Peters, W. Ranson, M. Sutton, T. Chu and J. Anderson, "Application of digital correlation methods to rigid body mechanics," *Optical Engineering,* vol. 22, no. 6, pp. 738-743, 1983.

[30] Z.-H. He, M. Sutton, W. Ranson and W. I. Peters, "Two dimensional fluid velocity measurements by use of digital speckle correlation techniques," *Experimental Mechanics,* vol. 24, no. 2, pp. 117-121, 1984.

[31] T. Chu, W. Ranson, M. Sutton and W. I. Peters, "Application of digital image correlation techniques to experimental mechanics," *Experimental Mechanics,* vol. 25, no. 3, pp. 232-245, 1985.

[32] M. Sutton, M. Cheng, W. Peters, Y. Chao and McNeill SR, "Application of an optimized digital correlation with the Newton Raphson method for partial differential corrections," *Image and Vision Computing,* vol. 4, no. 3, pp. 143-150, 1986.

[33] S. McNeill, W. I. Peters and M. Sutton, "Estimation of stress intensity factor by digital image correlation," *Engineering Fracture Mechanics,* vol. 28, no. 1, pp. 101-112, 1987.

[34] M. Sutton and Y. Chao, "Measurement of strains in a paper tensile specimen using computer vision and digital image correlation part I: data acquisition and image analysis system," *Journal of Korea Technical Association of the Pulp and Paper Industry,* vol. 70, no. 3, pp. 173-175, 1988.

[35] Y. Chao and M. Sutton, "Measurement of strains in a paper tensile specimen using computer vision and digital image correlation, part II: tensile specimen test," *Journal of Korea Technical Association of the Pulp and Paper Industry,* vol. 70, no. 4, pp. 153-156, 1988.

[36] H. Bruck, S. McNeill, M. Sutton and W. I. Peters, "Determination of deformations using digital image correlation with the Newton Raphson method for partial differential corrections," *Experimental Mechanics,* vol. 29, no. 3, pp. 261-267, 1989.

[37] P. Luo, Y. Chao, M. Sutton and W. I. Peters, "Accurate measurement of three dimensional deformations in deformable and rigid bodies using computer vision," *Experimental Mechanics,* vol. 33, no. 2, pp. 123-133, 1993.

[38] P. Luo, Y. Chao and M. Sutton, "Application of stereo vision to 3-D deformation analysis in fracture mechanics," *Optics Engineering,* vol. 33, no. 3, pp. 981-990, 1994.

[39] J. Helm, S. McNeill and M. Sutton, "Improved 3-D Image correlation for surface displacement measurement," *Optics Engineering,* vol. 35, no. 7, pp. 1911-1920, 1996.

[40] S. McNeill, J. Helm, J. Lan and M. Sutton, "Experimental evaluation of surface deformations in three areas of a Boeing 727 aircraft due to internal pressure and tail loading," USC ME-1-1997, 1997.

[41] H. Schreier, J. Braasch and M. Sutton, "Systematic errors in digital image correlation caused by intensity interpolation," *Optics Engineering,* vol. 39, no. 11, pp. 2915-2921, 2000.

[42] H. Lu and D. Cary, "Deformation measurements by digital image correlation: implementation of a second order displacement gradient," *Experimental Mechanics,* vol. 40, no. 4, pp. 393-400, 2000.

[43] H. Schreier and M. Sutton, "Systematic errors in digital image correlation due to undermatched subset shape functions," *Experimental Mechanics,* vol. 42, no. 3, pp. 303-310, 2002.

[44] Y. Wang, M. Sutton and H. Schreier, "Quantitative error assessment in pattern matching: effects of intensity pattern noise, interpolation, subset size and image contrast on motion measurements," *Strain,* vol. 45, pp. 160-178, 2009.

[45] Y.-Q. Wang, M. Sutton, X.-D. Ke, H. Schreier, P. Reu and T. Miller, "On error assessment in stereo-based deformation measurements," *Experimental Mechanics,* vol. 51, no. 4, pp. 405-422, 2011.

[46] X.-D. Ke, H. Schreier, M. Sutton and Y.-Q. Wang, "Error assessment in stereo-based deformation measurements," *Experimental Mechanics,* vol. 51, no. 4, pp. 423-441, 2011.

[47] M. Sutton, "Computer vision-based, noncontacting deformation measurements in mechanics: a generational transformation," *ASCE Applied Mechanics Reviews,* 2013.

[48] M. Sutton and F. Hild, "Recent advances and perspectives in digital image correlation," *Experimental Mechanics,* vol. 55, no. 1, pp. 1-8, 2015.

[49] R. Ghorbani, F. Matta and M. Sutton, "Full-Field Deformation Measurement and Crack Mapping on Confined Masonry Walls using Digital Image Correlation," *Experimental Mechanics,* vol. 55, pp. 227-243, 2015.

[50] B. Pan, L. Yu, J. Yuan, Z. Shen and G. Tang, "Determination of Viscoelastic Poisson's Ratio of Solid Propellants using an Accuracy-enhanced 2D Digital Image Correlation Technique," *Propellants, explosives, Pyrotechnics,* vol. 40, pp. 821-830, 2015.

[51] M. A. Sutton, J.-J. Orteu and H. W. Schreier, Image for Correlation for Shape, Motion and Deformation Measurements: Basic Concepts, Theory and Applications, New York: Springer Science+Business Media, 2009.

[52] R. Janeliukstis and X. Chen, "Review of digital image correlation application to large-scale composite structure testing," *Composite Structures,* vol. 271, 2021.

[53] Y. Blikharskyy, N. Kopiika, R. Khmil, J. Selejdak and Z. Blikharskyy, "Review of Development and Application of Digital Image Correlation Method for Study of Stress-Strain State of RC Structures," *Applied Sciences,* vol. 12, 2022.

[54] Y. L. Dong and B. Pan, "A Review of Speckle Pattern Fabrication and Assessment for Digital Image Correlation," *Experimental Mechanics,* vol. 57, pp. 1161-1181, 2017.

[55] P. Reu, "The Art and Application of DIC; All about Speckles: Edge Sharpness," *Experimental Techniques,* vol. 39, pp. 1-2, 2015.

[56] B. Pan, Z. Lu and H. Xie, "Mean intensity gradient: An effective global parameter for quality assessment of the speckle patterns used in digital image correlation," *Optics and Lasers in Engineering,* vol. 48, no. 4, pp. 469-477, 2010.

[57] T. Hua, H. Xie, S. Wang, Z. Hu, C. Pengwan and Q. Zhang, "Evaluation of the quality of a speckle pattern in the digital image correlation method by mean subset fluctuation," *Optics and Lasers in Engineering,* vol. 43, no. 1, pp. 9-13, 2011.

[58] G. Crammond, S. Boyd and J. Dulieu-barton, "Speckle pattern quality assessment for digital image correlation," *Optics and Lasers in Engineering,* vol. 51, pp. 1368-1378, 2013.

[59] X.-Y. Liu, R.-L. Li, T.-H. Cheng, G.-J. Cui, Q.-C. Tan and G.-W. Meng, "Quality assessment of speckle patterns for digital image correlation by Shannon entropy," *Optik,* vol. 126, pp. 4206-4211, 2015.

[60] J. Park, S. Yoon, T.-H. Kwon and K. Park, "Assessment of speckle-pattern quality in digital image correlation based on gray intensity and speckle morphology," *Optics and Lasers in Engineering,* vol. 91, pp. 62-72, 2017.

[61] J. Song, J. Yang, F. Liu and K. Lu, "Quality assessment of laser speckle patterns for digital image correlation by a Multi-Factor Fusion Index," *Optics and Lasers in Engineering,* vol. 124, 2020.

[62] *Introduction to Digital Image Correlation for VICEDU StereoDIC Measurement System,* Correlated Solutions.

[63] M. Kalaitzakis, "Uncrewed Aircraft Systems for Autonomous Infrastructure Inspection," Doctor of Philosophy, Department of Mechanical Engineering, University of South Carolina, Columbia, South Caroline, 2022.

[64] "SNEED Coding Solutions, Inc.," 2022. [Online]. Available: https://sneedcoding.com/.

[65] "Bentsai Shop," Bentsai, 2022. [Online]. Available: https://www.bentsaishop.com/.

[66] VIC-3D Software Manual, Correlated Solutions.